MEASUREMENT

OF

DEEP CRUSTAL RESISTIVITIES

by

ARTHUR M. KELLY

B.Sc., St. Francis Xavier University
(1957)

SUBMITTED IN PARTIAL FULFILLMENT OF THE

REQUIREMENTS FOR THE DEGREE OF

MASTER OF SCIENCE

at the

MASSACHUSETTS INSTITUTE OF TECHNOLOGY
September, 1962

Signature of Author _____
Department of Geology and Geophysics, August 22, 1962

Certified by _____
Thesis Supervisor

Accepted by _____
Chairman, Departmental Committee on Graduate Students

MEASUREMENT OF DEEP CRUSTAL RESISTIVITIES

by

ARTHUR M. KELLY

Submitted to the Department of Geology and Geophysics on August 22, 1962 in partial fulfillment of the requirements for the degree of Master of Science.

ABSTRACT

Earth resistivity measurements are usually made using an applied current source, often a square wave. An optimum linear system is derived for the detection of a square wave. A synchronous system is also described. It is almost as good for signal detection, having a signal-to-noise gain of 27 as compared to 30 for the linear system, and superior in portability and ease of obtaining data. If one takes 1 mv/cps bandwidth/km as representative of average earth noise, the system can detect signals down to 40 microvolts.

Man-made conductors, such as fences, lying close to the measuring equipment can distort readings. An analytical solution for a fence, parallel to the line of measurements, is presented. The solution has been evaluated over fairly wide ranges of the variables, using a digital computer, and tables of results are included.

Finally, some field data is presented and discussed. The method is found to be very useful for mapping both horizontal and vertical variations in the conductivity structure and in the regional geology. Measurements were made at maximum dipole separation of 12 miles. No trend towards a change of resistivity with depth was found; using Schlumberger's curves an estimated minimum depth to a layer thick enough to cause such a trend and having a resistivity one one-hundredth that of the average surface value was found to be three miles.

Thesis Supervisor: Theodore R. Madden
Title: Associate Professor of Geophysics

ACKNOWLEDGEMENTS

The author wishes to express particular thanks to Professors Theodore Madden and Thomas Cantwell, his thesis supervisor and faculty advisor, respectively. Both of these gentlemen have been most patient and understanding and have rendered great assistance.

Gratitude is also due to those who assisted in collecting field data, namely Dr. David Greenwalt and Messrs. Francis Maher, William Sill, Alan Regier, Björn Conrad and Thomas Ising.

Professor Martin Schetzer of the Department of Electrical Engineering offered much valuable advice on Communication Theory problems. Neil Dulaney and William Thompson also contributed valuable aid.

Maps and other relevant data were supplied by the Massachusetts Turnpike Authority, which agency also kindly granted permission to collect data on their right-of-way.

During the academic year 1961-1962, the author was the grateful recipient of a fellowship from the Petroleum Research Fund of the American Chemical Society. Financial support was also received from Project NR-371-401 of the Office of Naval Research during the summer of 1962.

Finally, the author wishes to thank Mrs. Patricia Thompson, who interpreted his handwriting and typed the final copy; and his wife, Frances, who patiently suffered through the entire production, and to whom this work is lovingly dedicated.

TABLE OF CONTENTS

Page

APPENDICES

TABLES

FIGURES

INTRODUCTION

Determinations of electrical properties are most accurate and detailed when made with applied current sources, since the number of degrees of freedom in the interpretation of the measurements are reduced by controlling the location, strength and frequency of the source. The direct relationship between the measured voltages and the unknown resistivities presents the simplest interpretation problem, although even this problem is not simple when the resistivity structure is complex. The techniques of measuring earth resistivities on a relatively small scale are well known and in constant use. As the scale increases, however, the method becomes limited by problems of signal detection; these involve the large noise amplitudes encountered, rather than small signals. When the scale reaches measurements of hundreds of kilometers or more, the present state of the act is inadequate and one is forced to use the noise itself to analyse deep electrical properties.

This thesis reports or attempts to make large scale measurements by improving signal detection techniques. Successful measurements were made up to 20 kilometers without utilizing the maximum capabilities of the instrument.

Older measurements have relied mostly on "brute force" methods to produce signals large enough to be detected. With

improved receiving devices, the physical size of the sending system can be reduced, allowing better portability and more mobile operations. Detection problems are common these days in the communication sciences; their solutions usually involve correlation techniques. The original Gish-Rooney resistivity apparatus used such a technique. The method, although simple in concept, is powerful. The system described in Chapter I is an extension of the Gish-Rooney concept. Because of the peculiarities of alternating current flows, low frequencies must be used for deep resistivity probing; long time spans are therefore necessary in the detection scheme.

An interesting problem encountered in making field measurements is the determination of the effect of metal fences whose length is of the same order of magnitude as the dipoles used, or even of the entire spread. An analytic solution, made with the aid of certain simplifying assumptions, is presented in Chapter II, together with a simple model experiment.

Finally, a section of field data, taken as a test of the apparatus, is presented and discussed in Chapter III.

CHAPTER I

INSTRUMENTATION

1.0 The Optimum Linear System

Following Lee, 1960, we define an optimum linear system as one which produces minimum mean-square error, where the mean-square error is given as

$$\overline{\varepsilon^2(t)} = \lim_{T \to \infty} \frac{1}{2T} \int_{-T}^{T} \left[f_o(t) - f_d(t) \right]^2 dt \qquad 1.1$$

Minimizing this equation leads to the fact that the impulse response of the system must satisfy the Wiener-Hopf equation, viz: (Lee, 1960, pp. 364-369)

$$\varphi_{id}(\tau) = \int_{\infty}^{\infty} h_{opt}(\sigma)\, \varphi_{ii}(\tau - \sigma)\, d\sigma \qquad 1.2$$

$$\text{for } \tau \geq 0$$

where $\varphi_{id}(\tau)$ is the input-desired output cross-correlation; $h_{opt}(\sigma)$ is the optimum linear system impulse response and $\varphi_{ii}(\tau)$ is the input autocorrelation function.

In making resistivity measurements, square waves are often used for the input signal, for two reasons: (a) A low-frequency alternating current is desirable to avoid polarization effects (b) Square waves are easy to generate. Such a device is used in this project and will be discussed later.

It is necessary then to determine the required correlation functions for a square wave. The autocorrelation function and power density spectrum of a square wave of period 2 sec. are, respectively:

$$\varphi_{ii}(\tau) = \begin{cases} E^2(1 + 2\tau N) & 2N - 1 \leq \tau \leq 2N \\ E^2(1 - 2\tau N) & 2N \leq \tau \leq 2N + 1 \end{cases} \qquad N = 0, \pm 1, \pm 2, \ldots \qquad 1.3$$

$$\Phi_{ii}(\omega) = \sum_{N=0}^{\infty} \frac{2E^2}{N^2\pi^2} (1 - \cos N\pi)\,\delta(\omega - N\pi) \qquad 1.4$$

These are derived in Appendix A. We note in passing that a square wave has only odd harmonics. Intuitively, one might suspect that the optimum system will be one which filters out everything except these frequencies, that is, a so-called "comb" filter.

Now, let the desired output be the square wave. Then, since the input is this same square wave plus noise, we have

$$\varphi_{id}(\tau) = \overline{f_i(t)\, f_m(t + \tau)} \qquad 1.5$$

where $f_m(t)$ is the message. If the noise is $f_n(t)$, we have:

$$\varphi_{id}(\tau) = \overline{[f_m(t) + f_n(t)]\, f_m(t+\tau)}$$

$$= \overline{f_m(t) f_m(t+\tau)} + \overline{f_n(t) f_m(t+\tau)}$$

$$= \overline{f_m(t) f_m(t+\tau)} + \overline{f_n(t) f_m(t+\tau)}$$

$$\therefore \varphi_{id}(\tau) = \varphi_{mm}(\tau) + \varphi_{nm}(\tau) \qquad 1.6$$

The usual assumption that the noise and signal are uncorrelated is now made. This being the case, $\varphi_{nm}(\tau) = 0$, and we find that

$$\varphi_{id}(\tau) = \varphi_{mm}(\tau) \qquad 1.7$$

For the input, we have:

$$\varphi_{ii}(\tau) = \overline{f_i(t) f_i(t+\tau)}$$

$$= \overline{[f_m(t) + f_n(t)]\ [f_m(t+\tau) + f_n(t+\tau)]}$$

$$= \overline{f_m(t) f_m(t+\tau)} + \overline{f_m(t) f_n(t+\tau)} + \overline{f_n(t) f_m(t+\tau)} + \overline{f_n(t) f_n(t+\tau)}$$

$$\varphi_{ii}(\tau) = \varphi_{mm}(\tau) + \varphi_{nm}(\tau) \qquad 1.8$$

again assuming no correlation between signal and noise.

Substituting 1.7 and 1.8 into 1.2, we obtain

$$\int_{-\infty}^{+\infty} h_{opt}(\sigma)\, \varphi_{mm}(\tau - \sigma)\, d\sigma + \int_{-\infty}^{+\infty} h_{opt}(\sigma)\, \varphi_{nn}(\tau - \sigma)\, d\sigma = \varphi_{mm}(\tau) \qquad \tau \geq 0 \qquad 1.9$$

as the necessary and sufficient conditions for minimum mean-square error.

The power density spectrum of a square wave resists factorization; fortunately, the Weiner-Hopf equation, 1.9, in this case can be solved heuristically. We know that any solution is unique (Lee, 1960).

We also know that a square wave has only odd harmonics. Hence, a system that filters out all but these harmonics is a good starting point.

Lee (1960) shows that a tapped delay line picks out harmonics of all orders. Hence, a tapped delay line, which is tapped twice in each period, with alternate signs at the output of the taps, should select only even harmonics as the number of taps becomes infinite. That is, let

$$h(t) \cong \frac{1}{K+1}\left[\delta(t) - \delta\left(t-\tfrac{T}{2}\right) + \delta\left(t-2\tfrac{T}{2}\right) - \delta\left(t-3\tfrac{T}{2}\right) + \cdots - \cdots \quad (-1)^K \delta\left(t-K\tfrac{T}{2}\right)\right.$$

$$= \frac{1}{K+1}\sum_{n=0}^{K}(-1)^n \delta\left(t - n\frac{T}{2}\right)$$

1.10

Substituting this expression in the Wiener-Hopf equation, 1.9, we find:

$$\int_{-\infty}^{+\infty} \frac{1}{K+1} \sum_{n=0}^{K} (-1)^n \, \delta\left(\sigma - n\frac{T}{2}\right) \varphi_{nn}(\tau - \sigma)\, d\sigma + \int_{-\infty}^{+\infty} \frac{1}{K+1} \sum_{n=0}^{K} (-1)^n \, \delta\left(\sigma - n\frac{T}{2}\right) \varphi_{mm}(\tau - \sigma)\, d\sigma = \varphi_{mm}(\tau) \qquad \tau \geq 0$$

$$\therefore \frac{1}{K+1} \sum_{n=0}^{K} (-1)^n \varphi_{nn}\left(\tau - n\frac{T}{2}\right) + \frac{1}{K+1} \sum_{n=0}^{K} (-1)^n \varphi_{mm}\left(\tau - n\frac{T}{2}\right)$$

$$= \varphi_{mm}(\tau) \qquad \tau \geq 0$$

1.11

Since $\varphi_{mm}(\tau)$ is a periodic function, the second term on the left hand side is simply $\varphi_{mm}(\tau)$. Also, since $\varphi_{nn}(\tau)$ is the autocorrelation function of random noise, it is a monotonically decreasing function; hence, as N becomes larger, this term approaches zero. This term represents the error. Thus, we see that for an infinite number of taps, we obtain a system with zero error. By making the number of taps large, we can make the error as

small as is necessary.

This system cannot, of course, be realized with an actual tapped delay line. However, the same effect can be achieved by sampling the function every half period (say, using a digital voltmeter with punched-card output) and programming a digital computer to perform the required averaging operations.

The transfer function of this system is shown in Appendix B to be:

$$H_{opt}(\omega) = \frac{1 - \exp(-\frac{jnT\omega}{2})}{1 + \exp(-\frac{jT\omega}{2})} \qquad 1.12$$

and its modulus to be:

$$\left| H(\omega) \right| = \left| \frac{\sin \frac{n\omega}{2}}{\cos \frac{\omega}{2}} \right| \qquad 1.13$$

A plot of equation 1.13 for n 20 is shown in figure 1.1.

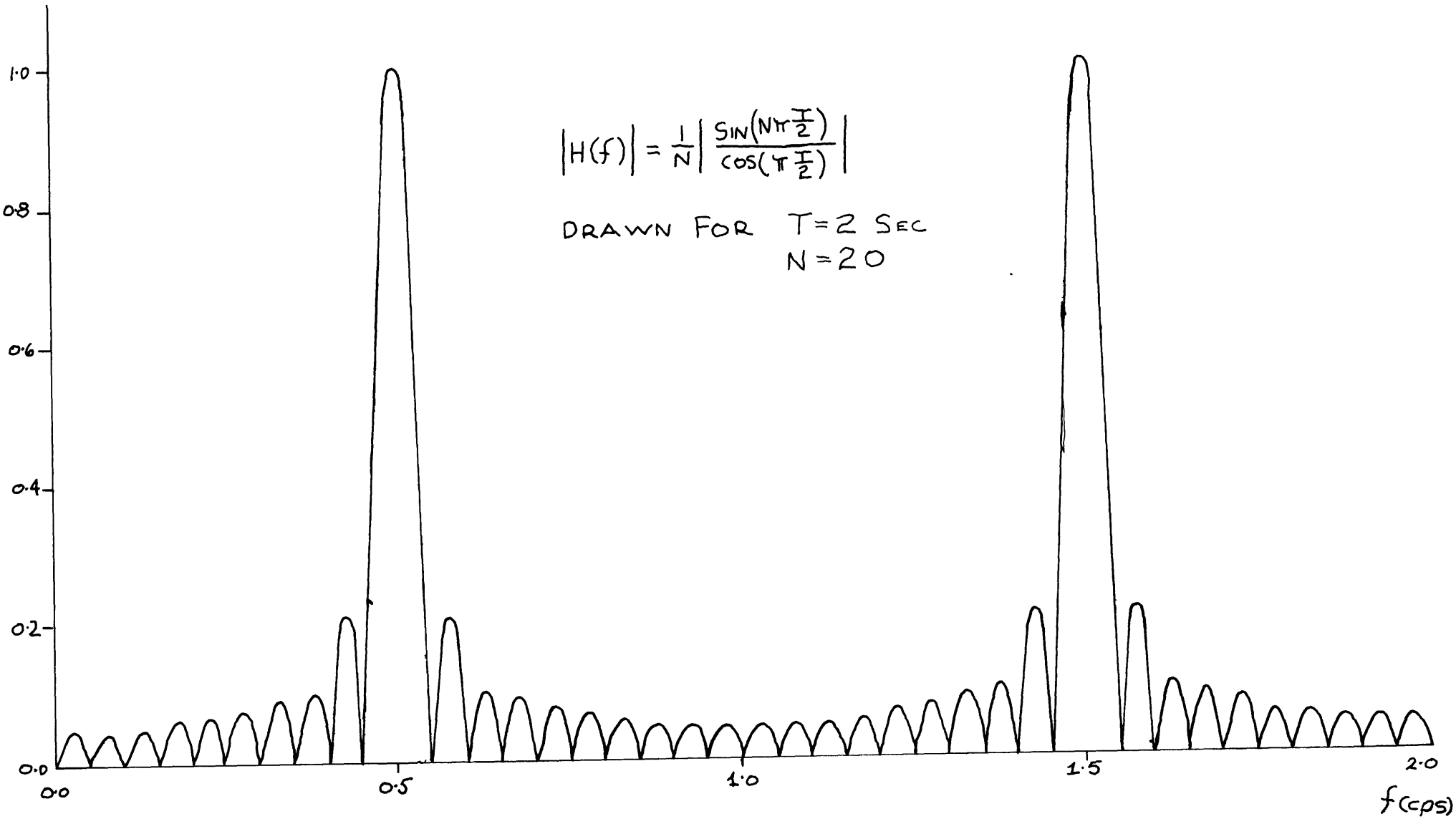
$|H(f)| = \frac{1}{N}\left|\frac{\sin(N\pi\frac{T}{2})}{\cos(\pi\frac{T}{2})}\right|$
DRAWN FOR T=2 SEC
N=20
1·0
0·8
0·6
0·4
0·2
0·0
0·0
0·5
1·0
1·5
2·0
f (cps)

FIG. 1·0

1.1 Signal - to - Noise Gain of the Optimum Linear System

Lee (1960) shows that, for a periodic sampling method, the gain in signal-to-noise ratio, assuming the period of the sampling function to be long enough to ensure independence of the noise components of the samples, is:

$$G = 10 \log_{10} (n) \text{ db.} \qquad 1.14$$

where n is the number of samples. Hence, for, say, $n = 1000$, we have

$$G = 10 \log (1000) \text{ db.}$$

$$= 30 \text{ db.} \qquad 1.15$$

If then, R is the input RMS noise to RMS signal ratio,

$$30 \text{ db.} = 20 \log v$$

or $$v = 32 \qquad 1.16$$

indicating that the maximum tolerable ratio of noise to signal at the input is about 30, if we are to detect the signal.

1.2 A Synchronous System

This system involves phase sensitive detection of the received signal with respect to a control signal which is synchronized to the sending current by means of time signals put out by W. W. V. The phase sensitive detector output is essentially the zeroth lag correlation of the received signal plus the noise with the control signal. The received signal and control signal are both square waves synchronized together so that they give a net correlation. The noise is uncorrelated with the control signal and it contributes only fluctuations to the phase detector output. The magnitude of these fluctuations is reduced in accordance to the length of time that is used to average the detector output, the exact relationship having a $t^{\frac{1}{2}}$ dependence. The existance of solid state amplifiers with input impedances of 10^9 ohms makes it possible to design such a receiving system, using battery operated electronic circuits packaged in a small case, capable of achieving averaging times of 1000 seconds. Some prefiltering of the received signals is also incorporated to reduce the noise to within the linear response region of the detector system.

The sending system is also designed with solid state devices, so that a portable system results. It can deliver up to 2 amperes into the ground at 400 volts, the current being reversed in synchronism with W. W. V. time signals,

so that remote correlation with the receiver detector can be achieved. The power is provided by a 1 KW 400 cps motor generator. A more detailed description and analysis of the system is given below.

Sender

The overall sender system block diagram is shown in Figure 1.2.

Power for the sender is drawn from a 115 volt 400 cycle motor generator set. The current is regulated by means of a series connected saturable reactor current regulator, then rectified. The resulting regulated d.c. is then converted to a square wave by means of a switching circuit using silicon controlled rectifiers (S. C. R.'s). This current switching stage is controlled by a flip-flop (S. C. R. driver circuit) which is inductively coupled to the S. C. R.'s. The flip-flop is in turn driven by an external pulse generator, running at 1 p.p.s. After switching, the current is passed through a current monitor. The output voltage activates a neon bulb so that the switching can be observed.

Receiver

The overall receiver system block diagram is shown in Figure 1.3.

The incoming signal is band passed through an RC low-

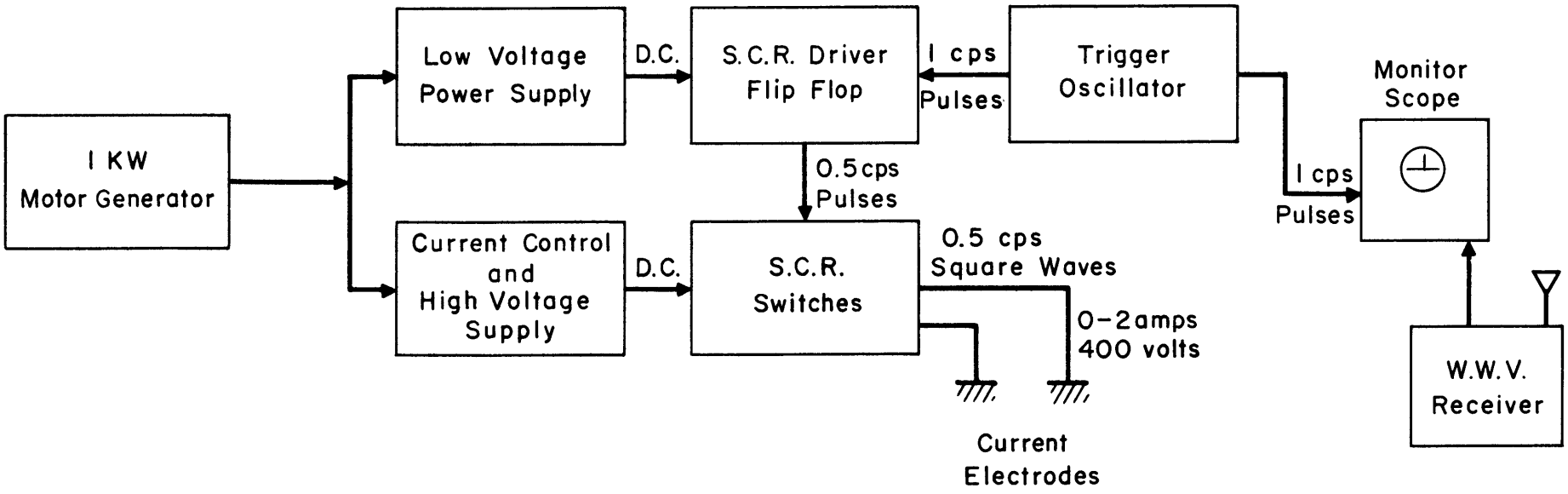

FIG. 1.2 DEEP RESISTIVITY SENDER : BLOCK DIAGRAM

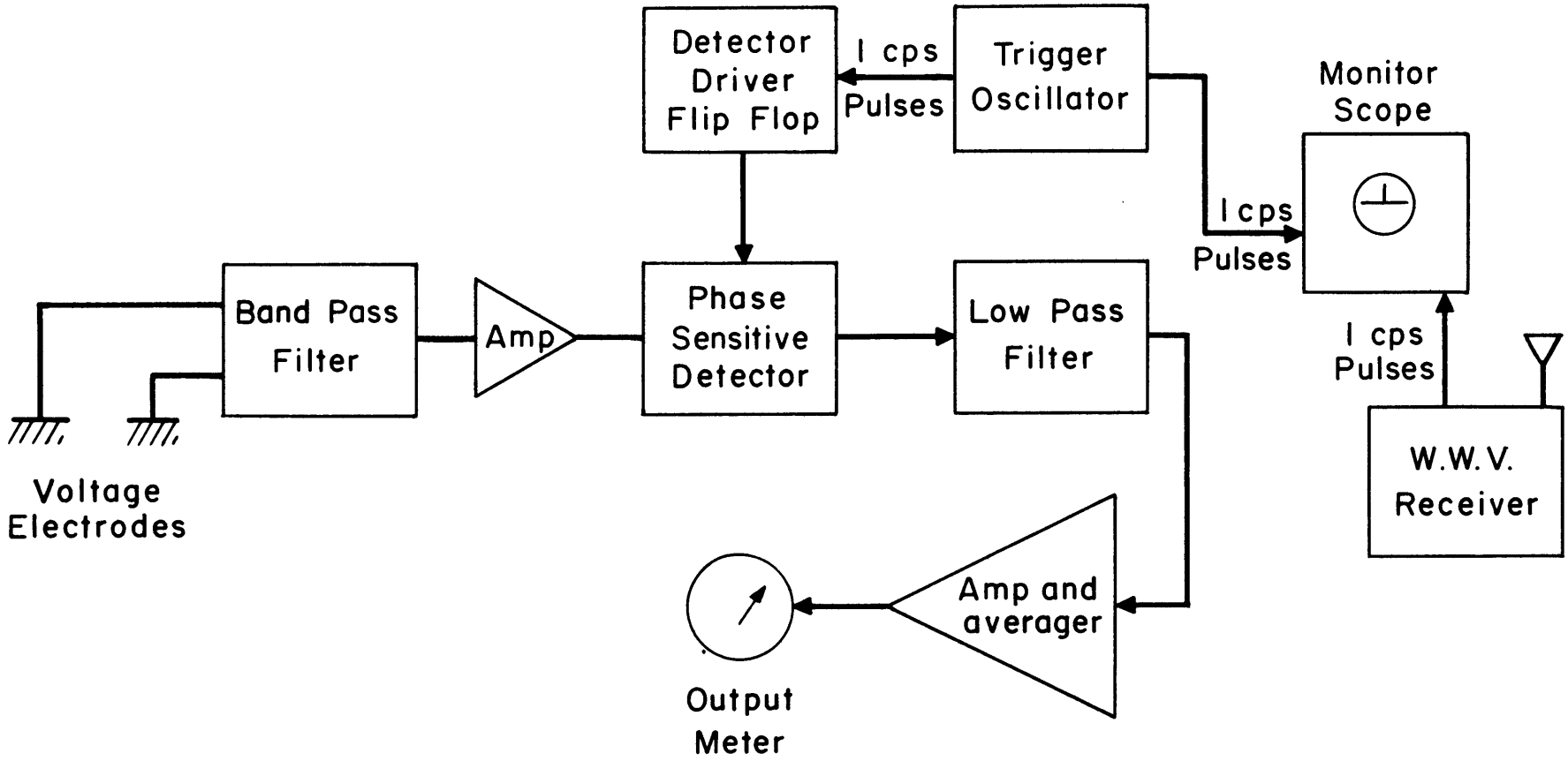

FIG 1.3 DEEP RESISTIVITY RECEIVER: BLOCK DIAGRAM

pass filter, a constant k, m-derived lowpass LC filter, and a three stage active RC highpass filter having Butterworth characteristics. The first stage of low-pass filtering was found necessary due to saturation of the first amplifier caused by large, modulated RF signals picked up on the long receiving wire. Buffer stages, (emitter follower amplifiers with a gain of 1) are used to unload the various filter stages.

The signal is then amplified or attenuated so as to have a maximum level of about 50 mv. A Philbrick model PA-2 operational amplifier is used.

Following this, the signal is switched by the phase-sensitive detector, which acts as a reversing switch. In the absence of noise and assuming all harmonics of the square wave to be present, its output would be pure d.c. However, due to the loss of some harmonics in the filters, the square wave is distorted and a fluctuating d.c. results.

The output of the phase sensitive detector is then passed through a three stage lowpass RC filter. The average value of this signal over pre-determined periods of from 30-1000 sec. is then evaluated by a Miller Integrator circuit, which also acts as an amplifier with a gain of 100. The result is read on a meter.

The circuit diagrams are shown in Figures 1.4 and 1.5.

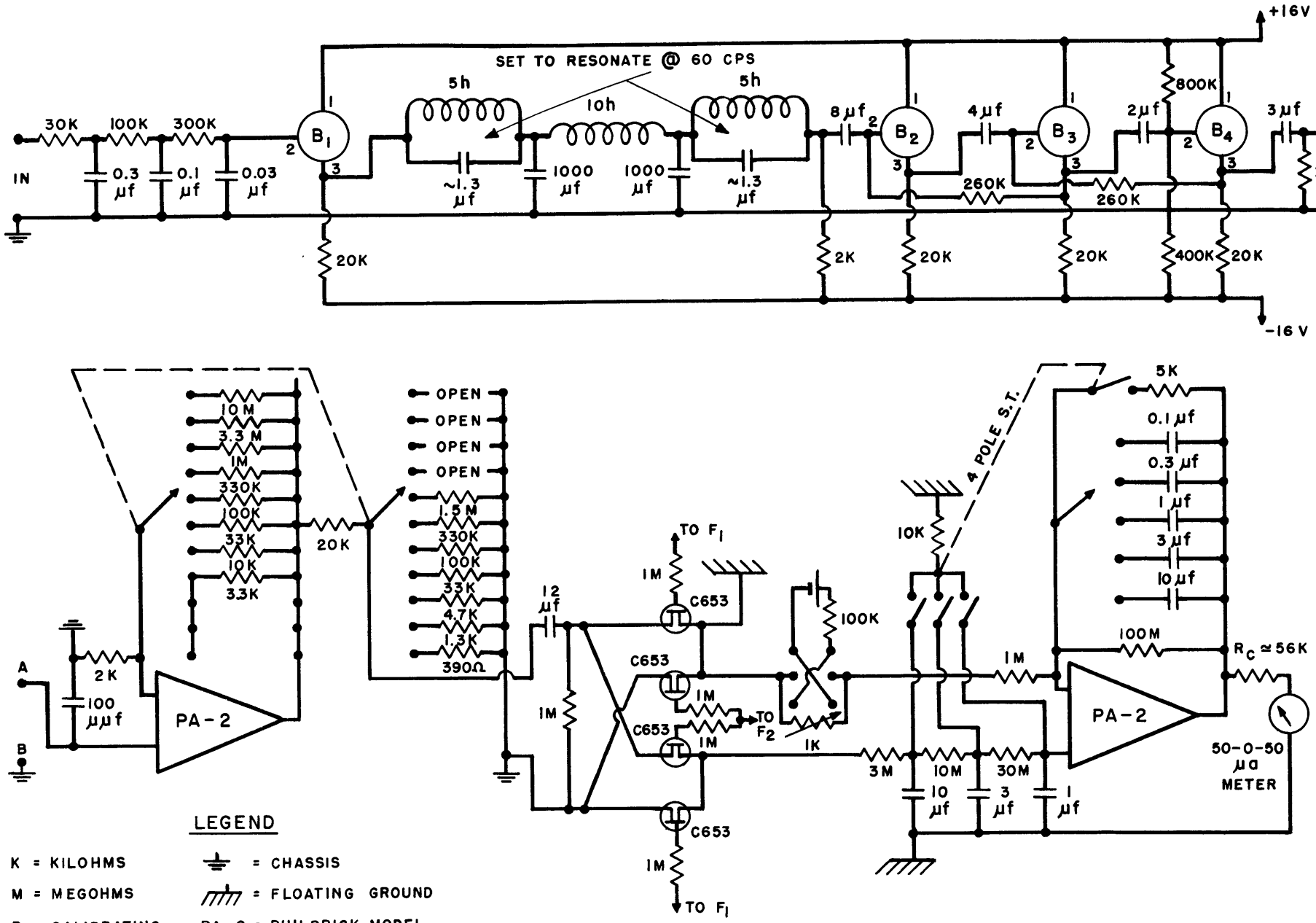

FIG. 14 SYNCHRONOUS RESISTIVITY RECEIVER

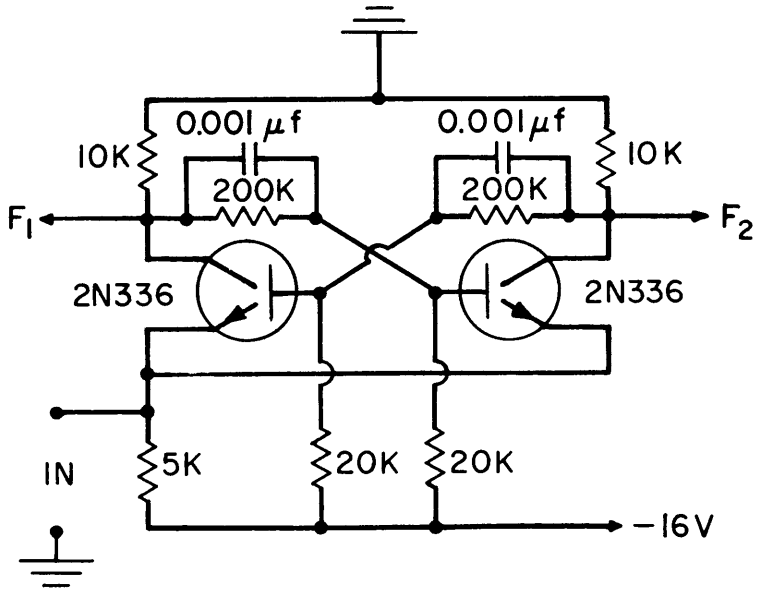

FLIP.-FLOP

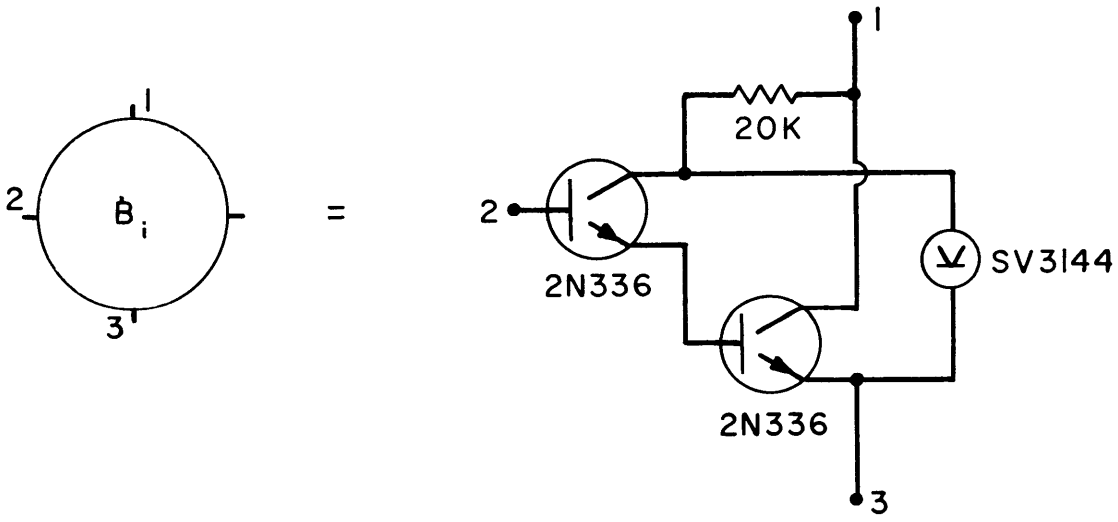

BUFFER

FIG. 1.5

Synchronization

Both sender and receiver are triggered by external pulse generators at a nominal rate of 1 pps. The pulse generators also are arranged to trigger the sweep of an oscilloscope, on which is displayed the 1 sec. pulses from W. W. V.; these are derived from special radio receivers. Both oscilloscopes are set at a sweep rate of 10 msec/cm. The pulse generators have adjustable rates, and they are set so as to fire 50 msec. before the W. W. V. pulses. The receiver output will change about 10% if the synchronization deviates 50 msec. from the standard setting, but it was found to be easy to keep the synchronization within 10 msec. The pulse generators used were temperature compensated unijunction pulse oscillators; crystal oscillators are being constructed for future measurements.

1.3 Signal-to-Noise Gain of the Synchronous System

In order to study the signal discrimination power of the receiver we can trace through what happens to noise which is assumed to have a unit power density spectrum, ignoring any amplification which effects both signal and noise equally. Figure 1.6 shows the noise amplitude (R. M. S.) after passing through the input band pass filters. These filters are used to reduce the noise fluctuations to within the linear response region of the amplifier circuits that follow. 60 cycles must be heavily discriminated against, as it may be hundreds of times bigger than the signal levels. These filter sections can handle up to 10 volts of 60 cycle noise without having the receiver output affected. If the amplifier sections had infinite dynamic range, these filter sections would not be necessary as we shall see.

The real filter action of the receiver is based on the phase sensitive detection and low pass filtering of the detector output. The detector reverses the signal every half cycle which essentially produces a signal that has a frequency which is the difference between the original frequency and the switching frequency. The power density spectrum of this output is shown in Figure 1.7. The dip at 0.5 cps represents the lack of any D. C. in the input to the detector because of the action of the band pass filter. The sender signal will be represented by D. C.

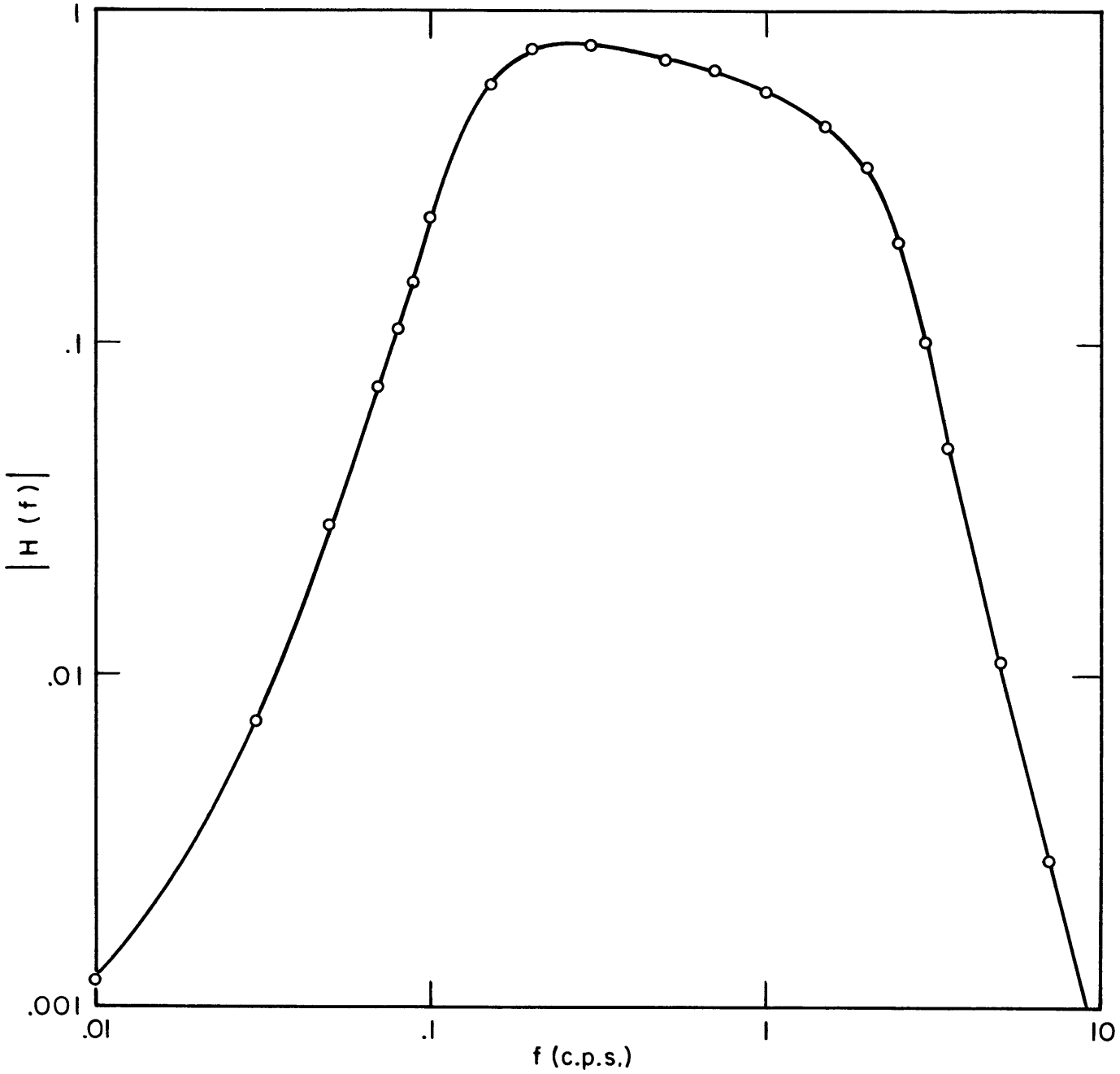

FIG. 1.6 TRANSFER FUNCTION - FIRST THREE STAGES

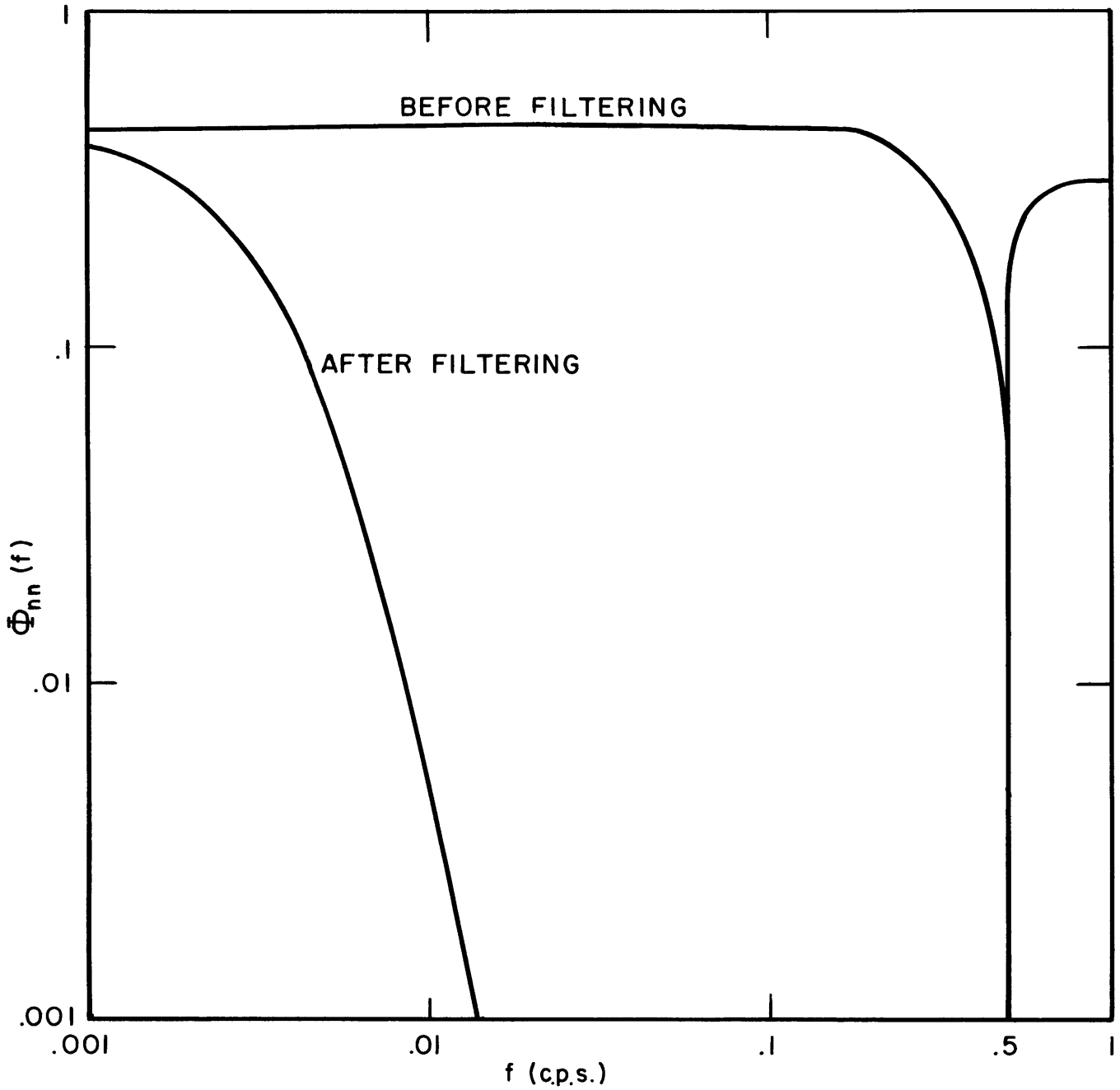

FIG. 1.7 POWER DENSITY SPECTRUM OF PHASE-SENSITIVE DETECTOR OUT PUT

at the detector output, so that low pass filtering of the detector output will reduce the noise while passing the signal. The effect of the three section low pass filter which follows the detector is also shown in Figure 1.7. A final stage of low pass filtering is achieved with the integrator circuit which essentially averages the detector output over a time determined by the RC constant of the circuit. Several settings are allowed, the longest integration time being 1000 seconds. The final noise spectrum after this integration is shown in Figure 1.8. The area under the curves shown here determine the mean (fluctuations)^2 of the output meter reading caused by the noise. Since the frequencies depicted in Figure 1.8 represent the difference frequency, we can see that only noise in a very narrow frequency band around 0.5 cps can affect the receiver. Table I shows the total power in the noise for various damping times. These figures were obtained by graphical integration.

The overall effect of the signal to noise discrimination can be expressed by the comparison of the noise power density necessary to cause meter fluctuations equivalent to a given signal amplitude. At 1000 second damping a 30 mv R. M. S. noise per unit bandwidth at 0.5 cps gives a fluctuation whose R. M. S. value equals that of a 1 mv signal. If we take a value like 1 mv/km/cps as a representative noise

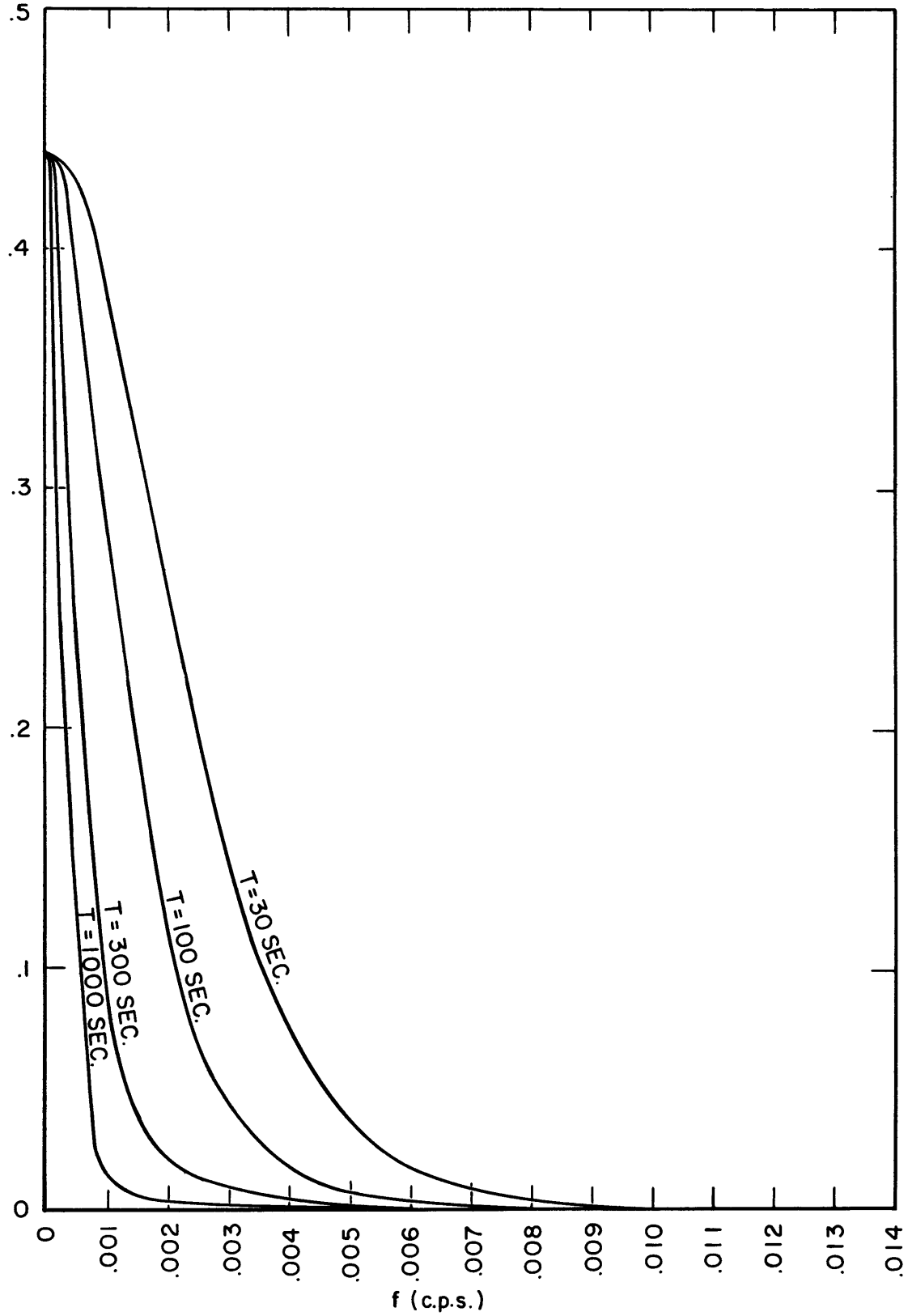

FIG. 1.8 FINAL POWER DENSITY SPECTRUM OF PHASE-SENSITIVE DETECTOR OUTPUT AFTER AVERAGING WITH MILLER INTEGRATOR

figure for igneous areas, one should be able to work with signals down to 0.1 mv/km.

In Figures 1.9 and 1.10 the effectiveness of such filtering is demonstrated in comparison to a visual identification of the signal in the noise.

A complete analysis of the phase-sensitive detector is given in appendix C.

The noise discrimination is achieved at the expense of time, and it takes the receiver about $2\frac{1}{2}$ min + 3 X the integrator time constant to reach 90% of its final reading. At the 1000 second setting this means one has to wait over 45 minutes before attempting to read the signal amplitude.

TABLE I

Damping Time (sec)	30	100	300	1000
Output S/N Ratio	10	13.5	19	27

(The output S/N ratio is computed assuming input RMS noise amplitude per cps bandwidth equals input signal amplitude)

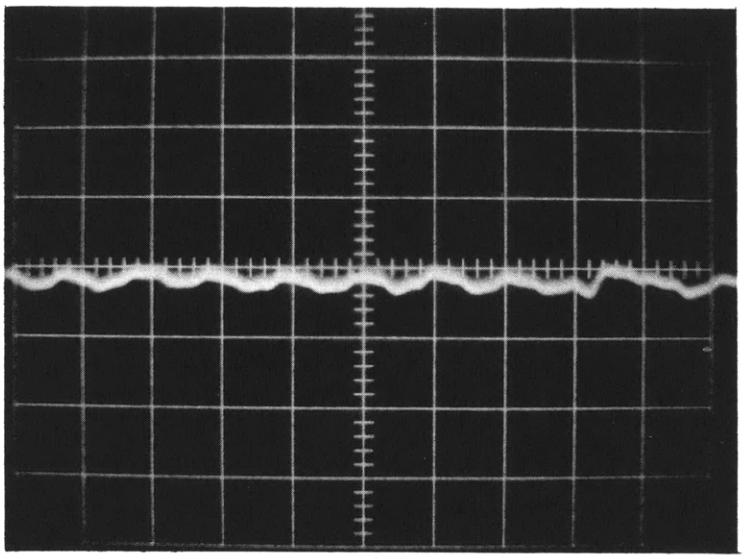

2 SEC/DIVISION

FIG. 1.9 SIGNAL AT OUTPUT OF 1st AMPLIFIER STAGE EQUIVALENT TO FULL SCALE METER DEFLECTION (SOME NOISE ALSO PRESENT)

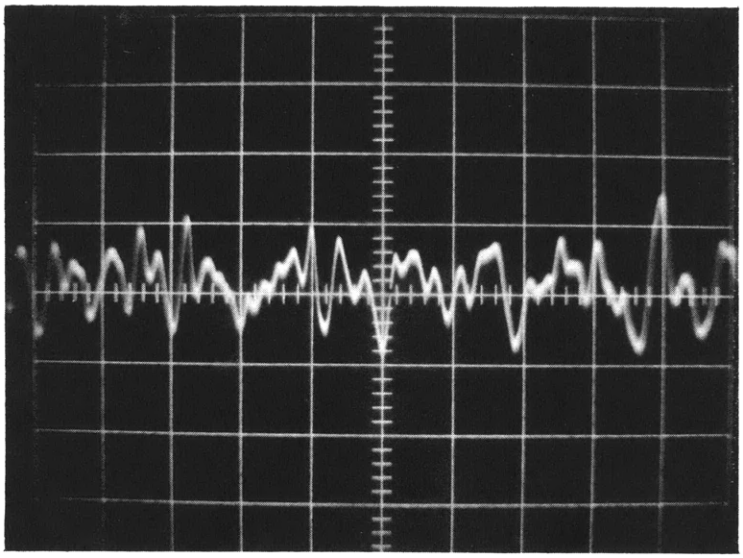

2 SEC/DIVISION

FIG. 1.10 SIGNAL AND NOISE AT OUTPUT OF 1st AMPLIFIER STAGE EQUIVALENT TO FULL SCALE METER DEFLECTION ± 10% 300 SECOND INTEGRATION TIME

Limitations imposed by dynamic range of system

Some further noise discrimination can be achieved by recording the output readings at regular intervals, and then using numerical low pass operators to reduce the fluctuations in the data. This method is limited however because of the finite range of the meter, which cannot distinguish between voltages that are greater than its maximum setting. The same sort of limitations hold throughout the system, as the whole analysis was based on the assumption that the amplifiers and filters were linear devices.

One of the first difficulties in field trials of the equipment was inteference from radio broadcasts. This turned out to be due to non linearities in the L. C. filter which demodulated the radio signals and produced large low frequency fluctuations. An RC low pass filter had to be added to prevent this from occuring.

The first amplifier stage is limited to 10 volts for its output, so that the amount of noise that can be handled has another restraint aside from the output fluctuations. The present system requires 50 mv of signal at the output of this stage to give a full scale meter deflection, so that the 10 volt limit appears adequate in terms of the amount of noise that can be handled by the filters that follow. The final amplifier can handle signals more than twice those needed for full scale meter readings, so that it is adequate

for the present system. The most critical limitation is thus the output meter itself, and if further noise discrimination is desired, a recorder of wider dynamic range will be needed.

CHAPTER II

THE FENCE PROBLEM

2.0 Description of the Problem

The long (1 mile or greater) lengths of wire that must be laid to make these measurements are such that it is often difficult (at least in densely populated areas) to find suitable areas of operation, since it is desirable to minimize wire breakages and interference with or by other people. Limited-access highways, such as the Massachusetts Turnpike are usually quite straight, do not have crossroads and are bounded by high fences which stop animals from getting on or over the highway. The verges of these roads are usually about 100 feet wide; hence these are good areas for resistivity work. However, these same fences are usually metal and are unbroken except at overpasses, underpasses, interchanges and some bridges. In general, the unbroken lengths average between one-half and one and one-half miles. It is desirable to know the effect of such a fence.

2.1 Analytical Solution

A perturbation technique is used to solve the problem. The method is the same as that followed by Regier (1962), except that a finite, rather than infinite, fence is considered here. The following assumptions are made:

(a) The fence effect is small.

(b) The effect is localized to a small zone along the fence.

(c) The resistance of the fence is near zero and hence the potential of any section of fence is an average of the continuously varying grounded potential along its length.

The third assumption implies that, in general, there will be a difference in potential between the fence and the ground near it. Consequently, the fence posts will act as current sources or sinks. Kirchoff's law holds, so if the fence "contact resistivity" (defined below) is known, the strength of these sources or sinks can be computed.

An important relation here is that which gives the potential due to a point source in a half-space. It is

$$V_o = \frac{I \rho_a}{2\pi r} \qquad 2.1$$

where

V_o = unperturbed potential

I = current

ρ_a = apparent resistivity of half-space

r = radial distance from the source.

In cartesian coordinates, if the source is located at the origin and a fence runs from (x_1,d) to (x_2,d), the imperturbed potential along the fence is:

$$V_o(x,d) = \frac{I \rho_a}{2\pi(x^2 + d^2)^{\frac{1}{2}}} \qquad 2.2$$

The potential of the fence, V_o is then the average of 2.2 from x_1 to x_2, viz:

$$V_F = \frac{I \rho_a}{2\pi(x_2 - x_1)} \int_{x_1}^{x_2} \frac{dx}{(x^2 + d^2)^{\frac{1}{2}}} \qquad 2.3$$

evaluating this expression, we find:

$$V_F = \frac{I \rho_a}{2\pi(x_2 - x_1)} \ln \frac{(x_2 + \sqrt{x_2^2 + d^2})}{(x_1 + \sqrt{x_1^2 + d^2})} \qquad 2.4$$

where $\ln x = \log_e x$.

We now define the fence contact resistivity, ρ_F, as the contact resistance times the length. Essentially, this is the contact resistance of a unit length. Using this definition, the differential current source strength due to an infinitisimal length of fence, dx, can be expressed by:

$$dI_F = \frac{V_o(x,d) - V_F}{\rho_F} dx \qquad 2.5$$

The effect of this current at a point on the x-axis, x_p,

will be to add a perturbing potential, V_p. The sign of V_p will be the same as dI_p. The relationship between has the same form as equation 2.1:

$$dV_p = \frac{\rho_a}{2\pi} \frac{dI_p}{\left[(x_r - x)^2 + d^2\right]^{\frac{1}{2}}} \qquad 2.6$$

where $\left[(x_r - x)^2 + d^2\right]^{\frac{1}{2}}$ is the distance from dx to the point $(x_r,0)$. Integrating this expression over the length of the fence, we have

$$V_p = \frac{\rho_a}{2\pi} \int_{x_1}^{x_2} \frac{dI_p}{\left[(x_r - x)^2 + d^2\right]^{\frac{1}{2}}} \qquad 2.7$$

as the expression for the perturbing potential.

Substituting from 2.2, 2.4 and 2.5, equation 2.7 becomes:

$$V_p = \frac{I \rho_a}{4\pi^2 \rho_p} \left[\int_{x_1}^{x_2} \frac{dx}{(x^2 + d^2)^{\frac{1}{2}} \left[(x_r - x)^2 + d^2\right]^{\frac{1}{2}}} - \frac{1}{x_2 - x_1} \ln \frac{(x_2 + \sqrt{x_2^2 + d^2})}{(x_1 + \sqrt{x_1^2 + d^2})} \int_{x_1}^{x_2} \frac{dx}{\left[(x_r - x)^2 + d^2\right]^{\frac{1}{2}}} \right] \qquad 2.8$$

For dipole-dipole coupling, if the sources are designated 1 and 2 and the receiving electrodes 1 and 2 as in the sketch below,

the expression for the received voltage is

$$V_R = V_{11} + V_{21} - V_{12} - V_{22} \qquad 2.10$$

where the first subscript refers to the source, the second to the receiver; i.e., V_{12} is the potential at receiving electrode number 2 due to source number 1. Since the apparent resistivity is directly proportional to the developed voltage, we may write, for dipole-dipole coupling,

$$\frac{\Delta \rho_a}{\rho_a} = \frac{V_p}{V_o} = \frac{V'_{11} + V'_{21} - V'_{12} - V'_{22}}{V_{11} + V_{21} - V_{12} - V_{22}} \qquad 2.11$$

where V_{ij} is the unperturbed potential and V'_{ij} the perturbing potential, at receiving electrode j due to source i.

This expression (2.11) was evaluated for ranges of d from 10 to 100, x_2 from -3000 to +30,000; fence lengths from 100 to 100,000; and for dipole spacings from 10,000 to 25,000; using in every case dipole lengths of 5000, and a ρ_a/ρ_f ratio of 0.1. The units are not stated since the end result is dimensionless. The computation was done

using an IBM 709 high speed digital computer. The results are tabulated in Appendix E.

2.2 A Model Experiment

In an attempt to check on the theoretical solution, the following experiment was performed:

A large open field was chosen, and two 50-foot dipoles laid out with their centres 100 feet apart. A current of 200 ma. at 20 cps was passed through one dipole; the voltage across the other was found to be 37 mv peak-to-peak. Using the formula

$$\rho_a = \frac{V}{I}\,\pi\,4[a(n^2-1)] \qquad 2.11$$

for dipole-dipole coupling, the apparent resistivity was found to be 1740 ohm-feet.

A row of 5 inch nails, 2 feet apart, was then driven into the ground, parallel to and at a distance of 10 feet from, the dipole line. The row was 350 feet long and symmetric about the dipole line. About 1 pint of NaCl solution was poured over each nail. The nails were then interconnected with no. 26 bare copper wire. (see sketch below)

The apparent resistivity measurement was then repeated; this time a figure of ρ_a 1462 ohm-feet was obtained, representing a difference of 16%. (To check this, the no-fence voltage was measured again the next day - the result was the same as before.)

The contact resistance of the fence was then measured

by driving two separate nails in the ground at one end, and, using an ordinary ohmmeter, measuring the resistance between the fence and each of the nails in turn, then between the two nails. If N_1, N_2, F represent the contact resistance of the nails and the fence respectively, we have:

$$F + N_1 = R_1$$

$$F + N_2 = R_2$$

$$N_1 + N_2 = R_3 \qquad 2.12$$

where R_1, R_2, R_3 are the measured values. These equations can then be solved for F. This measurement was repeated at the other end of the fence. Table II shows the measurements.

TABLE II

		$F + N_1$	$F + N_2$	$N_1 + N_2$
West end	a	550	950	1600
	b (leads reversed)	750	1000	1500
	mean	650	975	1550
East end	a	700	800	1500
	b (leads reversed)	750	520	1200
	mean	725	660	1350

These data gave values of 38 ohms and 17 ohms respectively

for the ends of the fence, the average being 27 ohms. Since the fence was 350 feet long, we have

$$\rho_F = 27 \times 350 \quad 9800 \text{ ohm-feet}$$

Thus, $\rho_a / \rho_F = .18$. This gives, when substituted into equation 2.9, a 43% fence effect, contrary to the original assumption that the fence effect is small, and also at variance with the measured fence effect. However, if we consider Table II, it is seen that the contact resistance of the nails is at least an order of magnitude larger than that of the fence. Also, S.P. effects disturb field measurements made with an ohmmeter. The discrepancy, therefore, is probably due to the method of measuring the fence resistance. In order to ensure that the ρ_a / ρ_F ratio is reliable, it will be necessary to devise a better method of measuring fence contact resistances. Unfortunately, time did not permit the author to do so for this model experiment.

CHAPTER III

FIELD MEASUREMENTS

3.0 Measurement Sites

In order to test the instrumentation, measurements were made along the Massachusetts Turnpike, between Framingham and Auburn, a distance of nearly 20 miles. (See Fig. 3.0) Hauck (1960) has reported on most of this area before, using one mile dipoles with a maximum centre-to-centre dipole separation of five miles.

Figure 3.0 shows the location of this stretch, together with the regional geology. This map was made from a larger one presented by Emerson (1917). As can be seen, the profile crosses three main rock types: i) the Milford granite, (rich in biotite), ii) The Westboro quartzite and iii) a large area of gneisses and schists of unknown composition and origin. Also, there are some narrow areas of the Brimfield schist, a rusty, graphitic, biotite schist of very low resistivity. (Hauck, 1960).

GEOLOGY AND LOCATION MAP

(AFTER EMERSON, 1917)

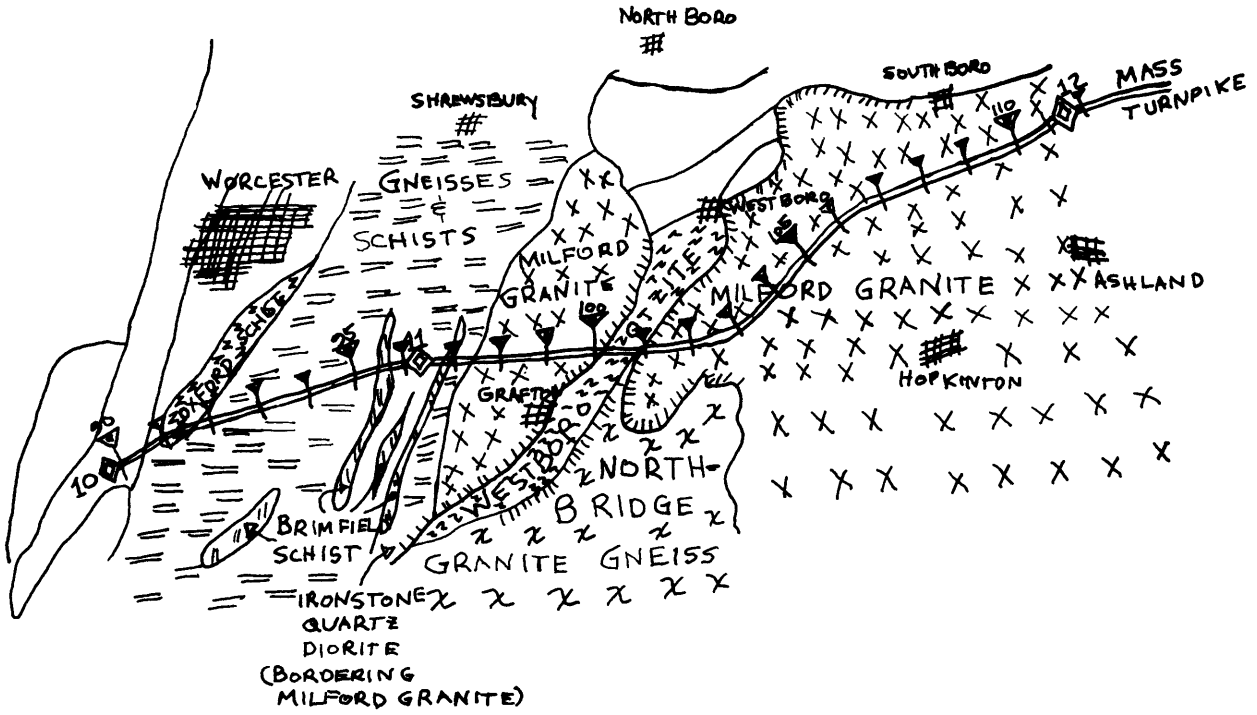

FIGURE 3.0

3.1 Field Procedure

The measurements were made using the dipole-dipole configuration described by both Haloff (1957) and Ness (1959). The signal is injected into the ground between two electrodes and the voltage measured between another pair some distance away. (Figure 3.1)

Fig. 3.1

The distance between the dipoles and the position of the whole array are varied in some convenient manner so as to obtain data points for a range of dipole spacings over the area under study. In practise, two contiguous dipoles are laid out for both sender and receiver; these require only three electrodes. The instrument is positional in the centre in such a manner that it may be connected to either of its two dipoles.

The data reported herein were obtained using dipole lengths of two miles with centre-to-centre separations of from four to twelve miles. Two vehicles, each manned by a crew of two were used. Communications were maintained using two-way radios; power was derived from small motor-

generator sets. In this manner, from four to twelve data points a day were obtained; the number depends on the weather, experience of the personnel and the number of times per diem that the wires were broken by animals or inquisitive or unwary humans. The most irritating and time-consuming problem in the field is broken wires. Number 26 stranded copper wire, coated with PVC was used; this does not have much mechanical strength. However, a heavier, stronger wire would be too unwieldy to use without mechanical devices to lay and retrieve it.

In addition to measuring the apparent resistivities, measurements were made of the contact resistances of the sections of fence along the turnpike. The average distance of the fence from the profile line was 100 feet; it was sometimes greater than this, but very seldom less. A General Radio model 1640A impedance bridge, with an external bias circuit to buck out self potentials, was used. The procedure was to measure, at each break in the fence, the resistance between each fence end and the guard rail and between the two fence ends. (See Fig. 3.2, below)

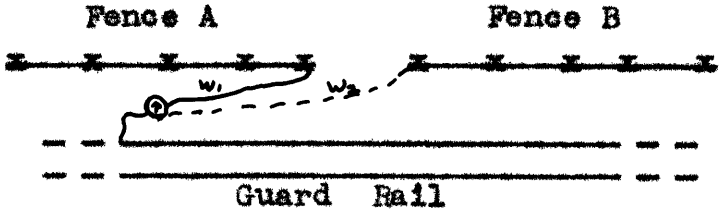

Fig. 3.2

Then,

$$R_A + R_G + W_1 = R_1$$

$$R_B + R_G + W_2 = R_2$$

$$R_A + R_B + W_1 + W_2 = R_3 \qquad 3.0$$

where R_A, R_B and R_G are the contact resistances of the fences and guard rail, respectively; W_1 and W_2 the resistances of the wires used; R_1, R_2 and R_3 are the measured values. Simultaneous solution of these equations gives the desired fence contact resistances. Measurements were made at both ends of each fence section and the results averaged. The product of the contact resistance of each fence section and its length then gives its contact resistivity. The results of the measurements are summarized in Table III.

TABLE III

FENCE CONTACT RESISTIVITIES

Fence Section	Length (km.)	R_A (Ω)	R_B (Ω)	$\bar{R}$	ρ_F (Ω m)
105.0-103.9	1.68	14.0	4.0	9.0	15.3×10^3
103.9-103.5	0.64	21.9	19.5	20.7	13.2
103.5-103.2	0.48	3.4	4.9	4.2	1.99
103.2-102.6	1.04	3.0	-	3.0	3.12
102.6-100.9	2.64	4.4	4.9	4.7	12.3
100.9-100.0	1.44	6.0	7.5	6.8	9.10
100.0- 99.4	0.96	14.4	7.5	10.9	10.5
99.4- 98.7	1.12	5.4	-	5.4	6.05
98.7- 98.1	0.96	-	3.4	3.4	3.28
98.1- 97.2	1.44	5.5	2.0	3.8	5.40
97.2- 96.9	0.48	5.9	6.4	6.2	2.95
96.9- 96.6	0.48	14.5	51.9	33.2	15.9
96.6- 96.5	0.16	3.0	-	3.0	1.28
96.5- 95.9	0.96	-	8.4	8.4	11.2
95.9- 95.6	0.48	13.5	10.0	11.8	5.65
95.6- 95.3	0.48	11.9	4.0	7.9	3.82
95.3- 94.5	1.28	17.9	-	17.9	2.30
94.5- 93.9	0.96	-	5.5	5.4	5.18
93.9- 93.6	0.48	3.5	45.0	24.3	11.6
93.6- 92.3	2.08	25.0	4.5	14.8	30.6
92.3- 91.7	0.96	1.5	9.5	5.5	5.28
91.7- 91.3	0.64	59.5	2.0	30.8	19.7

NOTES

(a) R_A and R_B are the contact resistances at back end of the section.

(b) No data was available on apparent resistivity near the surface, which would determine the ρ_a / ρ_f ratio. However, in general, the surface apparent resistivity will be lower than that at depth, due to rock weathering, moisture content of the soil, etc.

3.2 Presentation of Data

The apparent resistivities are computed using the equation

$$\rho_a = \frac{V}{I} \pi L(n(n^2 - 1)) \text{ ohmmeters} \qquad 3.1$$

where V and I are the voltage measured and the current sent, L is the dipole length in meters, n is the number of dipole lengths separating their centres. (This equation is only valid when both dipoles are the same length and their centres are separated by an integral multiple of this length). These values are then plotted in cross-section form, at the intersections of lines drawn downwards at 45 degree angles from the centres of the dipoles. The drawing is then contoured (often logarithmically), thus lending a two-dimensional character to the data. Figures 3.3 and 3.4 show the data and the contours.

No fence corrections were applied to these data since the effect was everywhere small and the data are only accurate to 10%.

The effect was determined using the values of ρ_a nearest the surface in order to determine ρ_a / ρ_f. The fence is divided into so many sections that complete determination of the cumulative effect is essentially impossible. Assuming that the longer sections will predominate, we note that there are only three sections longer than $\frac{1}{2}$ dipole

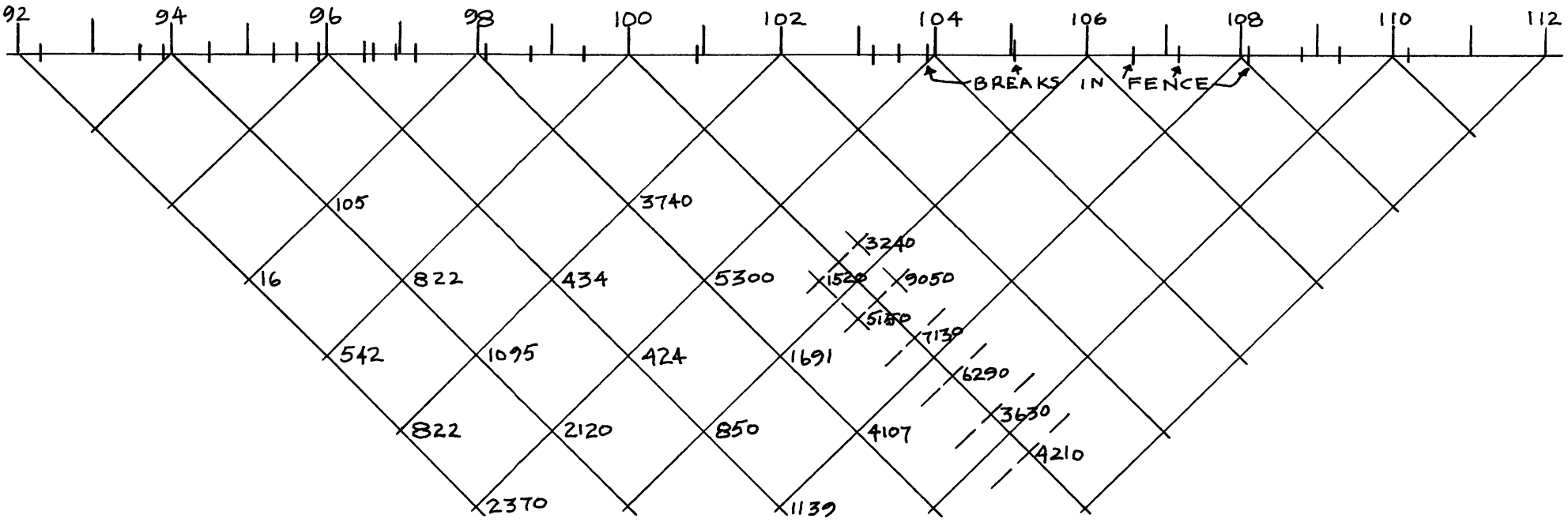

FIELD DATA

FIG. 3·3

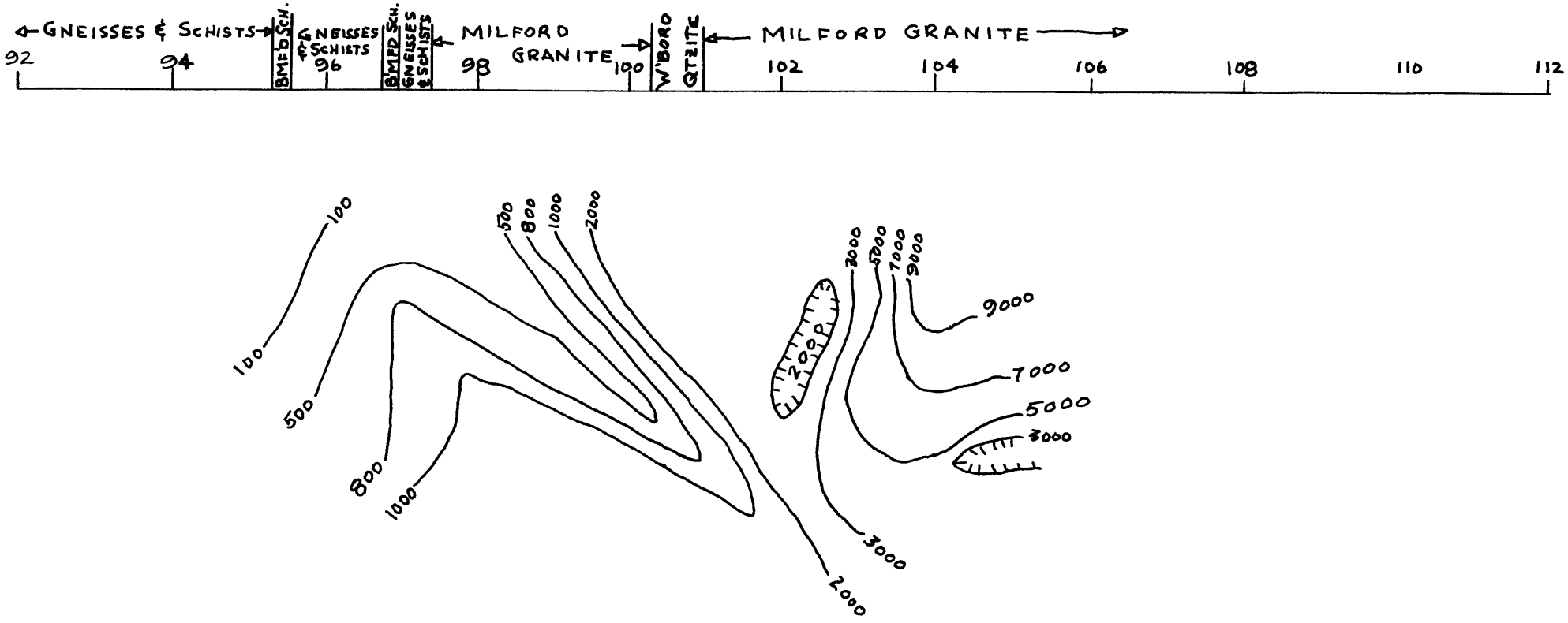

CONTOURED FIELD DATA
&
SURFACE GEOLOGY

FIG. 3.4

length, and none longer than 1.7 miles. The worst case is when sending from dipole 101-103 to dipole 97-99. In this case, the end of the fence is about 500 feet west of mile 101, and ρ_a/ρ_f is approximately 0.3. The fence is 1.7 miles long. Considering the fact that the dipoles are twice as long as those used for the theoretical solution, and using the tables in Appendix E, one can estimate the effect of such a fence to be of the order of a 20% increase in apparent resistivity.

3.3 Discussion of the Data

The data correlate well with the known geology as taken from Emerson's map. (The geologic divisions are shown with resistivity plots.) The low resistivities at the western end are caused by the presence of the Brimfield schist; as the array is moved easterly, onto the Milford granite, resistivities rise in a more or less uniform manner.

The diagonal extending down to the right from mile 96 shows anomalously low values at each intersection. Previous field work indicates that when anomalously low or high values are observed at every intersection of a diagonal, the cause is usually a surface effect, at or between the electrodes of the dipole in question.

In this case, the geology indicates the presence of linear stringers of Brimfield schist in a gneissic matrix, between miles 95 and 97, the electrode positions. Hand samples of this rock indicate resistivities as low as 77 ohmmeters, although such low values are rare for the samples taken from the outcrops. Regier(1962), who measured a selection of specimens in the laboratory, points out that these samples were weathered and rusted; this would tend to increase their resistivity, as the pyrite was weathered out. Fresh Brimfield schist, containing large amounts of pyrite, could very likely have resistivities of tens of ohm-meters or less.

CHAPTER IV

CONCLUSION

4.0 Instrumentation

The synchronous system, at its best, is approximately as good as the optimum linear system is for a sample size of 1000. One drawback is that for 1000 second damping, the synchronous system requires about 3000 seconds, or nearly an hour, to make one reading. However, this reading is the signal amplitude, whereas the optimum linear system requires that the field data be processed by a computer before being usable.

4.1 The Fence Problem

In general, the fence effect is small in most applications. Certain geometrics can, however, produce large effects. One in particular is the case where the fence length is of the same order of magnitude as the total electrode array and where one end of the fence is close to that receiver electrode which is nearest the sender. For example, for 5000 ft. dipoles, 10,000 feet apart with a 10,000 ft. fence so arranged that it extends from outside the sender to a point between the sending and receiving dipoles, the solution predicts effects of the order of 20 to 35%. These values are probably too large, as a perturbation analysis was used, but they are probably not far off.

4.2 Field Data

The method is useful for measuring horizontal as well as vertical variations of the earth's conductivity structure. In fact, determination of the structure at depth is not possible without measurements of the horizontal variation, because of surface effects. Therefore, measurements with a fixed sender position cannot, in general, be used to determine the deep conductivity structure.

A more important conclusion is that the data conform to the local geologic structure to the extent that deep resistivity profiling is a very useful technique for geological surveying.

There is no trend in these data which would indicate the presence of some extensive layered structure of significantly different resistivity below the known geologic structure. If we postulate the presence of a very thick layer of much lower resistivity, an estimate of its minimum depth may be made using the Schlumberger curver (La Compagnie General Geophysique, 1955). As an example, let this layer have a resistivity of one one-hundredth the average resistivity at the surface. Because of the wide scatter in the data, a change of as much as 50% in the observed apparent resistivity due to the postulated layer would be difficult to detect. If detectable as a trend, a change of 50% in

the deepest data points as compared to the average values near the surface, would indicate that the minimum depth of the layer is ½ the depth of the deepest observations, in this case about 3 miles or 5 km. The greater the scatter in the data, the more pronounced the trend must be in order to be detectable. This means that the estimated minimum depth to the layer must be decreased in proportion to the scatter for a given resistivity contrast.

4.3 Suggestions for Future Work

It is possible that the damping time of the last stage of the synchronous receiver could be increased another order of magnitude by using mylar or polystyrene capacitors. Such capacitors can now be manufactured in values of up to 100 microfarads while still having very high insulation resistance. This change will probably demand a more stable amplifier than is currently being used, so as to minimize drift effects. Another way to avoid drift problems might be to reduce the gain of individual stages while using a preamplifier to achieve the same overall gain.

More field measurements are needed in order to understand better the effect of horizontal variations of the conductivity structure on measurements made to determine vertical variation. Finally, it is suggested that large scale model experiments be conducted to check on the assumptions made in solving the fence problem analytically.

APPENDIX A

Autocorrelation Function and Power Density Spectrum of a Square Wave.

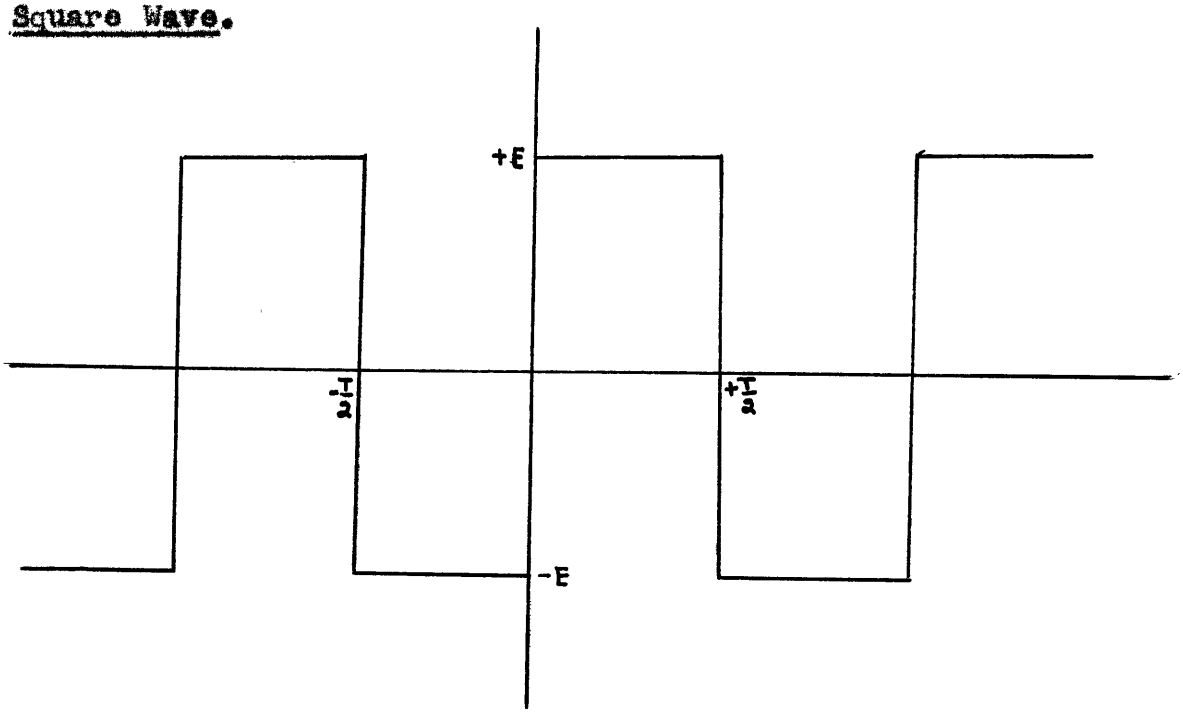

Fig. A-1

The definition of an autocorrelation function of a periodic function f(t) is:

$$\varphi_{ii}(\tau) = \frac{1}{T}\int_{-\frac{T}{2}}^{+\frac{T}{2}} f(t)f(t+\tau)dt \qquad \text{A.1}$$

where T is the period. The autocorrelation function of a periodic function is also periodic, with the same period and is an even function (Lee, 1960). Hence, we need only integrate over one period. Two distinct cases present themselves, viz:

$$0 \leq \tau \leq T/2$$

$$-T/2 \leq \tau \leq 0$$

Consider the first case:

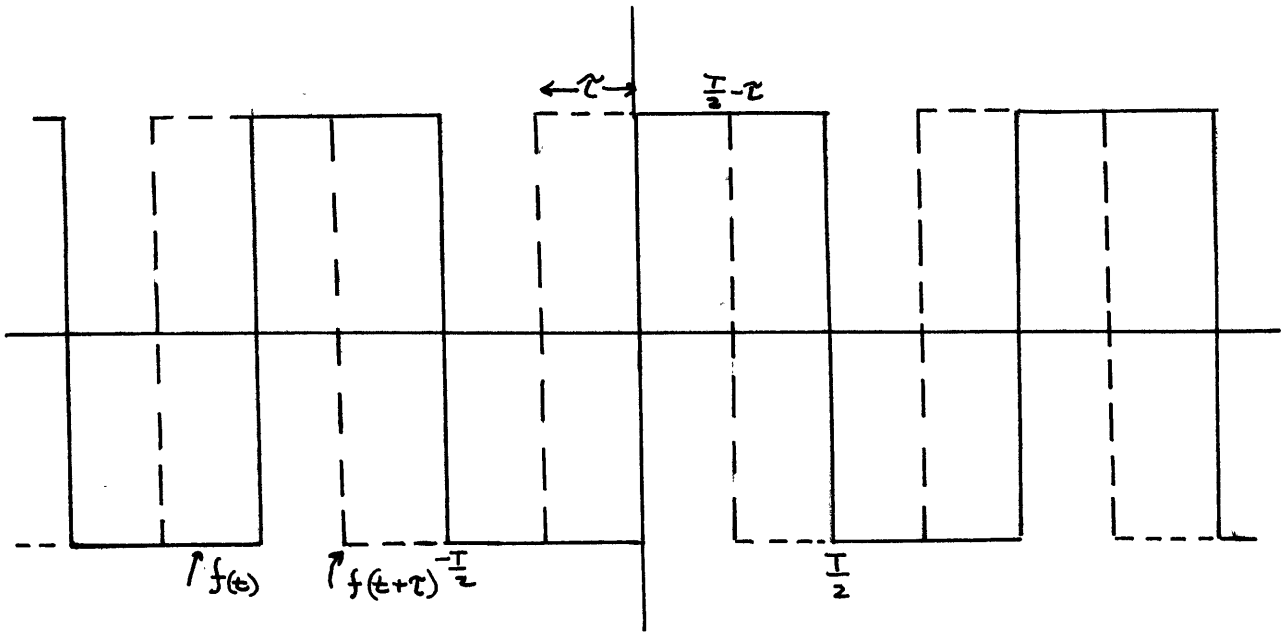

Fig. A-2

From Fig. A-2, :

$$\varphi_{11}(\tau) = \frac{1}{T}\int_{-\frac{T}{2}}^{-\tau} E^2 dt + \frac{1}{T}\int_{-\tau}^{0}(-E^2)dt + \frac{1}{T}\int_{0}^{\frac{T}{2}-\tau} E^2 dt + \frac{1}{T}\int_{\frac{T}{2}-\tau}^{\frac{T}{2}}(-E^2)dt$$

$$= \frac{E^2}{T}\left\{ t\Big|_{-\frac{T}{2}}^{-\tau} - t\Big|_{-\tau}^{0} + t\Big|_{0}^{\frac{T}{2}-\tau} - t\Big|_{\frac{T}{2}-\tau}^{\frac{T}{2}} \right\}$$

$$= \frac{E^2}{T}\left\{ -\tau + \frac{T}{2} - \tau + \frac{T}{2} - \tau - \frac{T}{2} + \frac{T}{2} - \tau \right\}$$

$$= \frac{E^2}{T}(T - 4\tau) \quad , \qquad 0 \le \tau \le T/2$$

A.2

The second case is $-\frac{T}{2} \leq \tau \leq 0$

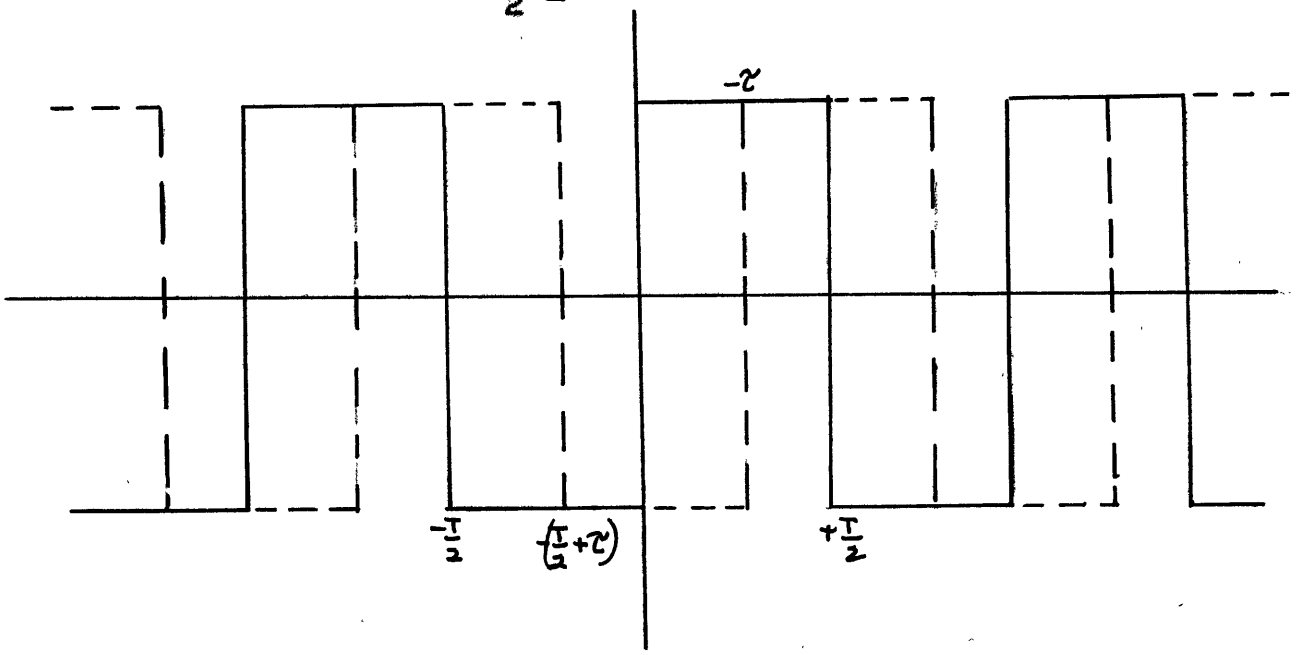

then

$$\rho_{11}(\tau) = \frac{1}{T}\int_{-\frac{T}{2}}^{-\frac{T}{2}-\tau}(-E^2)dt + \frac{1}{T}\int_{-\frac{T}{2}-\tau}^{0}E^2dt + \frac{1}{T}\int_{0}^{-\tau}(-E^2)dt + \frac{1}{T}\int_{-\tau}^{T/2}E^2dt$$

$$= \frac{E^2}{T}\left\{ -t\Big|_{-\frac{T}{2}}^{-\frac{T}{2}-\tau} + t\Big|_{-\frac{T}{2}-\tau}^{0} - t\Big|_{0}^{-\tau} + t\Big|_{-\tau}^{T/2} \right\}$$

$$= \frac{E^2}{T}\left\{ \frac{T}{2}+\tau \quad -\frac{T}{2}+\frac{T}{2}+\tau+\tau+ \quad \frac{T}{2}+\tau \right\}$$

$$= \frac{E^2}{T}\left(T+4\tau\right) \qquad -\frac{T}{2} \leq \tau \leq 0$$

Then:

$$\varphi_{11}(\tau) = \begin{cases} \frac{E^2}{T}(T + 4\tau) & (2n-1)\frac{T}{2} \leq \tau \leq (2n)\frac{T}{2} \\ & n = 0, \pm 1, \pm 2, \ldots \\ \frac{E^2}{T}(T - 4\tau) & (2n)\frac{T}{2} \leq \tau \leq (2n+1)\frac{T}{2} \end{cases}$$

A.3

Again by definition, the Power Spectrum of a periodic function f(t), whose autocorrelation function is $\varphi_{11}(\tau)$, is:

$$\underline{\Phi}_{ii}(n) = \frac{1}{T}\int_{-\frac{T}{2}}^{+\frac{T}{2}} \varphi_{ii}(\tau) e^{-jn\omega_o\tau}\, dt$$

A.4

(i.e., the Fourier Transform)

where n is the order of the harmonic when the fundamental frequency is ω_o. This is, of course, a line spectrum.

Since the autocorrelation function is an even function, we can use a cosine transform, viz:

$$\underline{\Phi}_{ii}(n) = \frac{1}{T}\int_{-\frac{T}{2}}^{\frac{T}{2}} \varphi_{ii}(\tau)\cos n\omega_o\tau\, d\tau$$

A.5

Performing the integration:

$$\underline{\Phi}_{ii}(n) = \frac{1}{T}\int_{-\frac{T}{2}}^{0} \frac{E^2}{T}(T + 4\tau)\cos n\omega_o\tau\, d\tau + \frac{1}{T}\int_{0}^{+\frac{T}{2}} \frac{E^2}{T}(T - 4\tau)\cos n\omega_o\tau\, d\tau$$

$$= \frac{E^2}{T^2}\left[T \int_{-\frac{T}{2}}^{0} \cos n\omega_0\tau\, d\tau + 4\int_{-\frac{T}{2}}^{0} \tau \cos n\omega_0\tau\, d\tau \right.$$

$$\left. + T \int_{0}^{\frac{T}{2}} \cos n\omega_0\tau\, d\tau - 4 \int_{0}^{\frac{T}{2}} \tau \cos n\omega_0\tau\, d\tau \right]$$

A.6

Note that

$$\int \cos ax\, dx = \frac{1}{a} \sin ax$$

$$\int x \cos ax\, dx = \frac{\cos ax}{a^2} + \frac{x \sin ax}{a}$$

hence A.6 reduces to:

$$\frac{E^2}{T^2}\left\{ T\left[\frac{\sin n\omega_0\tau}{n\omega_0}\right]_{-\frac{T}{2}}^{0} + 4\left[\frac{\cos n\omega_0\tau}{n^2\omega_0^2} + \frac{\tau \sin n\omega_0\tau}{n\omega_0}\right]_{-\frac{T}{2}}^{0} \right.$$

$$\left. + T\left[\frac{\sin n\omega_0\tau}{n\omega_0}\right]_{0}^{\frac{T}{2}} - 4\left[\frac{\cos n\omega_0\tau}{n^2\omega_0^2} + \frac{\tau \sin n\omega_0\tau}{n\omega_0}\right]_{0}^{+\frac{T}{2}} \right\}$$

$$= \frac{E^2}{T^2}\left[\frac{8}{n^2\omega_0^2}(1 - \cos n\omega_0 T/2) - \frac{2T \sin n\omega_0 T/2}{n\omega_0}\right]$$

Since $\omega_0 T = 2\pi$, this reduces to

$$\Phi(n) = \frac{2E^2}{n^2\pi^2}(1 - \cos n\pi)$$

A.7

The Power Density Spectrum can then be written as

$$\Phi(\omega) = \sum_{n=0}^{\infty} \frac{2E^2}{n^2\pi^2}(1 - \cos n\pi) U_0(\omega - n\omega_0)$$

A.8

Note that $1 - \cos n\pi = 0$ for n even.

APPENDIX B

The Transfer Function of a Tapped Delay Line

The linear system whose impulse response is:

$$h(t) = U_o(t) - U_o(t - \frac{T}{2}) + U_o(t - T) - U_o(t - \frac{3T}{2}) + \cdots - \cdots \qquad B.1$$

where $U_o(t)$ is the unit impulse function (or Dirac delta function) is a delay line with N taps, alternate taps having a change of sign in this case. The transfer function of a linear system is defined as the Fourier Transform of the impulse response, viz:

$$H(\omega) = \int_{-\infty}^{\infty} h(t) e^{-j\omega t} dt \qquad B.2$$

Note that

$$\int_{-\infty}^{\infty} U_o(t - kT) e^{-j\omega t} dt = e^{-j\omega kT} \qquad B.3$$

hence,

$$H(\omega) = 1 - e^{-j\omega T/2} + e^{-j\omega T} - e^{-j\omega 3T/2} + \cdots\cdots$$

$$= \sum_{n=0}^{N-1} (-1)^n e^{-jn\omega T/2} \qquad B.4$$

Equation B.4 can be written as the sum of two series,

$H_1(\omega)$ and $H_2(\omega)$, where:

$$H_1(\omega) = 1 + e^{-j\omega T} + e^{-2j\omega T} + e^{-3j\omega T} + \ldots$$
$$= \sum_{n=0}^{\frac{N}{2}-1} e^{-j(n)\omega T} \qquad \text{B.5}$$

$$H_2(\omega) = -e^{-j\omega T/2} - e^{-j\omega 3T/2} - e^{-j\omega 5T/2} - \ldots$$
$$= -\sum_{n=1}^{\frac{N}{2}} e^{-j\omega(2n-1)T/2} \qquad \text{B.6}$$

Equation B.6 can be further simplified by factoring out $e^{-j\omega T/2}$, i.e.;

$$H_2(\omega) = -e^{-j\omega T/2} \sum_{n=1}^{N/2} e^{-jn\omega T}\, e^{j\omega T} \qquad \text{B.7}$$

which, as a moment's thought will demonstrate, is the same as

$$H_2(\omega) = -e^{-j\omega T/2} \sum_{n=0}^{\frac{N}{2}-1} e^{-jn\omega T} \qquad \text{B.8}$$

Combining B.5 and B.8 we have:

$$H(\omega) = (1 - e^{-j\omega T/2}) \sum_{n=0}^{\frac{N}{2}-1} e^{-jn\omega T} \qquad \text{B.9}$$

The sum of a geometric series of ratio r with k terms is

$$S_k = \frac{1 - r^k}{1 - r} \qquad \text{B.10}$$

Using this relation, equation B.9 becomes:

$$H(\omega) = (1 - e^{-j\omega T/2}) \frac{1 - e^{jN\omega T/2}}{1 - e^{j\omega T}}$$

B.11

which reduces to

$$H(\omega) = \frac{1 - e^{-jN\omega T/2}}{1 \quad e^{-j\omega T/2}}$$

B.12

This expression can be expressed as the sum of the real and imaginary parts, by rationalizing. The result is

$$H(\omega) = \frac{1 + \cos \omega T/2 - \cos N\omega T/2 - \cos (N-1)\omega T/2}{2 + 2 \cos \omega T/2} + j \frac{\sin \omega T/2 + \sin N\omega T/2 + \sin (N-1)\omega T/2}{2 + 2 \cos \omega T/2}$$

B.13

If we square and add the real and imaginary parts, after some algebra the expression reduces to:

$$\left| H(\omega) \right|^2 = \frac{1 - \cos N\omega T/2}{1 + \cos \omega T/2}$$

B.14

The following trigonometric identities are useful:

$$1 + \cos x = 2 \cos^2 \frac{x}{2}$$

$$1 - \cos x = 2 \sin^2 \frac{x}{2}$$

B.15

Using the identities, B.15, we find

$$\left|H(\omega)\right|^2 = \frac{\sin^2 N\omega T/4}{\cos^2\left(\frac{\omega T}{4}\right)}$$

whence

$$\left|H(\omega)\right| = \left|\frac{\sin N\omega T/4}{\cos\left(\frac{\omega T}{4}\right)}\right| \qquad \text{B.16}$$

for $T = 2$ seconds,

$$\left|H(\omega)\right| = \left|\frac{\sin \frac{N\omega}{2}}{\cos \frac{\omega}{2}}\right| \qquad \text{B.17}$$

APPENDIX C

Analysis of the Receiving System

In order to simplify the analysis of the system, the transfer function of the first three filters was measured by the usual techniques. The results are shown graphically in Figure 1.6. Assuming white noise input to the system, i.e., $\Phi_{ii}(\omega) = \text{const} = N^2$, then the output power density spectrum is

$$\Phi_{oo}(\omega) = N^2 \left| H(\omega) \right|^2 \qquad C.1$$

where $H(\omega)^2$ is the square of the function shown in Figure 1.6.

Consider now the phase-sensitive detector. It can be thought of as a modulator, since it multiplies its input by a square wave of amplitude 1. Let $f_1(t)$ be the input to the modulator and $g(t)$ be the square wave. The output is then

$$f_o(t) = f_1(t)g(t) \qquad C.2$$

Now, the input is signal plus noise, i.e.:

$$f_1(t) = s(t) + n(t) \qquad C.3$$

hence

$$f_o(t) = s(t)g(t) + n(t)g(t) \qquad C.4$$

the autocorrelation of the output is then

$$\varphi_{oo}(\tau) = \overline{s(t)g(t)s(t+\tau)g(t+\tau)} + \overline{n(t)g(t)n(t+\tau)g(t+\tau)} \qquad C.5$$

Now define a new function $p(t) = s(t)g(t)$

then the first term on the right hand side becomes

$$\overline{p(t)p(t+\tau)} = \varphi_{pp}(\tau) \qquad C.6$$

In the second term on the right hand side, we can assume that n(t) and g(t) are statistically independent. Hence:

$$\overline{n(t)n(t+\tau)g(t)g(t+\tau)} = \overline{n(t)n(t+\tau)} \cdot \overline{g(t)g(t+\tau)}$$

$$= \varphi_{nn}(\tau) + \varphi_{gg}(\tau) \qquad C.7$$

whence

$$\varphi_{oo}(\tau) = \varphi_{pp}(\tau) + \varphi_{nn}(\tau)\varphi_{gg}(\tau) \qquad C.8$$

The power density spectrum is then:

$$\underline{\Phi}_{oo}(\omega) = \underline{\Phi}_{pp}(\omega) + \underline{\Phi}_{nn}(\omega) * \underline{\Phi}_{gg}(\omega) \qquad C.9$$

Now, since g(t) is a square wave, we can write its Fourier expansion as

$$g(t) = \sum_{-\infty}^{\infty} G_n e^{jn\pi t} \qquad C.10$$

where $G_n = \dfrac{\sin \frac{n\pi}{2}}{\frac{n\pi}{2}}$ $\qquad n = \pm 1, \pm 2, \ldots$

$= 0 \qquad n = 0$

(N. B. modulation frequency is 0.5 cps = π)

whence

$$\underline{\Phi}_{gg}(n) = |G_n|^2 \qquad C.11$$

and we can write

$$\underline{\Phi}_{gg}(\omega) = \sum_{-\infty}^{\infty} |G_n|^2 \delta(\omega - n\pi) \qquad C.12$$

Then

$$\underline{\Phi}_{nn}(\omega) * \underline{\Phi}_{gg}(\omega) = \int_{-\infty}^{\infty} \underline{\Phi}_{nn}(\omega - \sigma) \sum_{-\infty}^{\infty} |G_n|^2 \delta(\sigma - n\pi) d\sigma$$

$$= \sum_{n=-\infty}^{\infty} |G_n|^2 \underline{\Phi}_{nn}(\omega - n\pi) \qquad C.13$$

whence

$$\underline{\Phi}_{oo}(\omega) = \underline{\Phi}_{pp}(\omega) + \sum_{-\infty}^{\infty} |G_n|^2 \underline{\Phi}_{nn}\left(\frac{\omega}{2} - n\pi\right)$$

$$= \underline{\Phi}_{pp}(\omega) + 2 \sum_{n=1}^{\infty} \left(\frac{\sin \frac{n\pi}{2}}{\frac{n\pi}{2}} \right) \underline{\Phi}_{nn}(\omega - n\pi) \qquad C.14$$

To find $\underline{\Phi}_{pp}(\omega)$, write

$$g(t) = 2 \sum_{n=1}^{\infty} \frac{\sin \frac{n\pi}{2}}{\frac{n\pi}{2}} \cos(n\pi t) \qquad C.15$$

$$s(t) = \sum_{m=1}^{\infty} A_m \cos(m\pi t + \varphi_m) \qquad C.16$$

We write s(t) in this form since the first three filter stages cause amplitude and phase changes in the components of the input square wave.

Then

$$s(t)g(t) = 2 \sum_{m=1}^{\infty} \sum_{n=1}^{\infty} A_m \left(\frac{\sin \frac{n\pi}{2}}{\frac{n\pi}{2}} \right) \left[\cos(m\pi t + \varphi_m) \cos(n\pi t) \right] \qquad C.17$$

Using the trigonometric identity

$$\cos a \cos b = \tfrac{1}{2}\left[\cos(a+b) + \cos(a-b)\right] \quad \text{we get:}$$

$$s(t)g(t) = \sum_{m=1}^{\infty}\sum_{n=1}^{\infty} A_m\left[\frac{\sin\frac{n\pi}{2}}{\frac{n\pi}{2}} \cos\left[(m+n)\pi t + \varphi_m\right] + \cos\left[(m-n)\pi t + \varphi_m\right]\right] \qquad C.18$$

This signal has power only at discrete frequencies of $0, \pm\pi, \pm 2\pi, \ldots$. Since the next stage of low-pass filtering has a response which is less than -20 db at .01 cps (= $.02\pi$), in practice we need only consider the d.c. terms. These we get only when m = n.

Hence

$$s(t)g(t) \cong \sum_{n=1}^{\infty} A_n\left[\frac{\sin\frac{n\pi}{2}}{\frac{n\pi}{2}}\right] \cos\varphi_n \qquad C.19$$

As many terms of this equation as are necessary can be evaluated, since for a given square wave input amplitude A, we can find An and φn from Figures 1.6 and 1.7. It follows that

$$\underline{\Phi}_{oo}(\omega) = \left(\sum_{m=1}^{\infty} A_m\left[\frac{\sin\frac{m\pi}{2}}{\frac{m\pi}{2}}\right] \cos\varphi_m\right) \delta(\omega) + \sum_{k}\left(\frac{\sin\frac{k\pi}{2}}{\frac{k\pi}{2}}\right)^2 \cdot \underline{\Phi}_{nn}(\omega - k\pi)$$

$$k = \pm 1, \pm 2, \ldots \qquad C.20$$

An exact solution for the next stage is difficult to obtain. Hence, assume the three sections of the low-pass

filter do not load each other. Since the transfer functions for one stage is

$$H(s) = \frac{1}{RC(s + 1/RC)} \qquad C.21$$

The function for three stages, all with the same time constant is:

$$H(s) = \frac{1}{T^3(s + 1/T)^3} \qquad C.22$$

where $T = RiCi$

Since we are only interested in the amplitude response (the phase angles being random for the noise) we have

$$\left|H(\omega)\right| = \frac{1}{(1 + \omega^2 T^2)^{3/2}} \qquad C.23$$

The power density spectrum of the noise after this filter is shown in Figure 1.7.

The transfer function for the final stage is derived as follows. In the Philbrick PA-2 amplifier, used in the configuration shown below (Figure C.1)

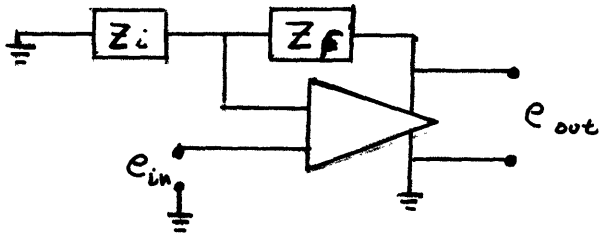

Fig. C.1

the manufacturer advises that the transfer function is

$$H(s) \cong 1 + \frac{Z_f(s)}{Z_1(s)} \qquad \text{C.24}$$

In our case, we have

$$Z_1 = R_1 \qquad T = R_f C$$

$$Z_f = \frac{R_f}{1 + sT} \qquad \text{C.25}$$

Therefore

$$H(s) = 1 + \frac{R_f}{R_1} \quad \frac{1}{1 + sT}$$

$$= \left[1 + \frac{R_f}{R_1}\right] \left[\frac{1 + \frac{sT}{1 + \frac{R_f}{R_1}}}{1 + sT} \right] \qquad \text{C.26}$$

Note that if Z_f were a pure resistance, we would have

$$H(s) = 1 + \frac{R_f}{R_1} = K, \text{ the gain of the amplifier at dc.}$$

Then, let

$$\frac{T}{K} = T'$$

Hence

$$H(s) = K \frac{1 + sT'}{1 + sT} \qquad \text{C.27}$$

Hence

$$H(j\omega) = K\left[\frac{1 + j\omega T'}{1 + j\omega T}\right]$$

$$= K\left[\frac{(1 + j\omega T')(1 - j\omega T)}{1 + \omega^2 T^2}\right]$$

$$= K\left[\frac{1 + \omega^2 TT'}{1 + \omega^2 T^2}\right] + jK\left[\frac{\omega(T' - T)}{1 + \omega^2 T^2}\right] \qquad C.28$$

recall that $T' = \frac{T}{K}$. Substituting,

$$H(j\omega) = K\left[\frac{1 + \frac{\omega^2 T^2}{K}}{1 + \omega^2 T^2}\right] + jK\left[\frac{\omega T(\frac{1}{K} - 1)}{1 + \omega^2 T^2}\right]$$

whence

$$\left|H(\omega)\right|^2 = K^2\left[\frac{1 + \frac{\omega^4 T^4}{K^2} + \frac{\omega^2 T^2}{K^2} + \omega^2 T^2}{(1 + \omega^2 T^2)^2}\right] \qquad C.29$$

Now $K = 10^2$ and the maximum value of T is 10^3. Figure 1.7 shows that we need not consider any ω larger than .03. Hence, the second and third term in the brackets are small compared to $\omega^2 T^2$ and we may write

$$\left|H(\omega)\right| \cong K\sqrt{\frac{1}{1 + \omega^2 T^2}} \qquad C.30$$

It is interesting to note that this is the same as a single stage of low-pass filtering. The advantage of using

this configuration is, however, that the high input impedance of the PA-2 amplifier (several hundred megohms) allows averaging times of up to 1000 secs. to be realized.

APPENDIX D

Evaluation of Fence Integrals

Equation 2.8, repeated here for reference, is:

$$V_p(X_r,0) = \frac{I\rho a^2}{4\pi^2\rho_f}\left[\int_{X_1}^{X_2}\frac{dx}{(x^2+d^2)^{\frac{1}{2}}\left[(x_r-x)^2+d^2\right]^{\frac{1}{2}}} - \frac{1}{x_2-x_1}\ln\frac{(x_2+\sqrt{x_2^2+d^2})}{(x_1+\sqrt{x_1^2+d^2})}\int_{X_1}^{X_2}\frac{dx}{\left[(x_r-x)^2+d^2\right]^{\frac{1}{2}}}\right]$$

2.8

Consider the expression under the second integral sign. Expanding the denominator, we have:

$$I_2 = \int_{X_1}^{X_2}\frac{dx}{\sqrt{x_r^2-2x_rx+x^2+d^2}}$$

D.1

whence I_2 indicates the second integral which can be written

$$I_2 = \int_{X_1}^{X_2}\frac{dx}{\sqrt{x^2-2x_rx+(x_r^2+d^2)}}$$

D.2

This integral can be found in most tables of integrals. Its evaluation leads to the expression

$$I_2 = \ln\frac{\left[\sqrt{(x_r-x_2)^2+d^2}+(x_2-x_r)\right]}{\left[\sqrt{(x_r-x_1)^2+d^2}+(x_1-x_r)\right]}$$

D.3

The first integral is an elliptic one, which transforms into (Franklin, 1944)

$$I_1 = C \int_{\phi_1}^{\phi_2} \frac{d\phi}{\sqrt{1 + k^2 \sin^2 \phi}} \qquad D.4$$

$$= C \left[F(k, \phi_2) - F(k, \phi_1) \right] \qquad D.5$$

where

$$C = \frac{p - q}{M^{\frac{1}{2}}}$$

$$k = \left(1 - \frac{N}{M}\right)^{\frac{1}{2}}$$

$$p = \frac{x_r + (x_r^2 + 4d^2)^{\frac{1}{2}}}{2}$$

$$q = \frac{x_r - (x_r^2 + 4d^2)^{\frac{1}{2}}}{2} \qquad D.6$$

$$M = \left[(q - x_r)^2 + d^2\right] \left(p^2 + d^2\right)$$

$$N = \left[(p - x_r)^2 + d^2\right] \left(q^2 + d^2\right)$$

$$\varphi = \tan^{-1} \left[\sqrt{-\frac{p}{q}} \left(\frac{x - q}{p - x}\right)\right]$$

$F(k, \phi)$ = elliptic integral of the first kind.

Tables of the function $F(k, \phi)$ may be found in many standard works such as Jahnke and Emde, Dwight, etc.

In order to gain a deeper insight into the effect, however, consider the following:

In general, the point at which we wish to know the

potential is some distance from the source, i.e.,

$$x_r \gg d \tag{D.7}$$

In this case, $C \cong \frac{1}{x_r}$ and $k^2 \cong 1$, as can be seen by inspection. I_2 then becomes

$$I_2 = \frac{1}{x_r} \int_{\phi_1}^{\phi_2} \frac{d\phi}{\sqrt{1 + \sin^2 \phi}} \tag{D.8}$$

$$= \frac{1}{x_r} \int_{\phi_1}^{\phi_2} \frac{d\phi}{\cos \phi}$$

$$= \frac{1}{2x_r} \ln\left(\frac{1 + \sin \phi}{1 - \sin \phi}\right)\Bigg]_{\phi_1}^{\phi_2} \tag{D.9}$$

Using the trigonometric identity

$$\sin\phi = \frac{\tan \phi}{\left[1 + \tan^2\phi\right]^{\frac{1}{2}}} \tag{D.10}$$

we find

$$I_2 = \frac{1}{2x_r} \ln \left(\frac{\sqrt{1 + \tan^2} + \tan \phi}{\sqrt{1 + \tan^2} - \tan \phi}\right) \tag{D.11}$$

Referring to equation D.6, we find that for $x_r \gg d$,

$$p \cong x_r \tag{D.12}$$

and

$$q \cong -\frac{d^2}{x_r} \tag{D.13}$$

Using D.12, D.13 and the definition of $\tan\phi$ from D.6:

$$I_2 = \frac{1}{2x_r}\left[\ln\frac{(\sqrt{1+X_2^2}+X_2)}{(\sqrt{1+X_2^2}-X_2)} - \ln\frac{(\sqrt{1+X_1^2}+X_1)}{(\sqrt{1+X_1^2}-X_1)}\right.$$

$$\text{where } X_1 = \frac{x_r x_1 + d^2}{d(x_r - x_1)} \qquad \text{D.14}$$

(The definition of X_1 is obtained by substituting D.12 and D.13 in the definition of $\tan\phi$ given in D.6)

The whole expression for the perturbing voltage is then:

$$V_p(x_r,0) =$$

$$\frac{I\rho_a^2}{4\pi^2\rho_F}\left\{\frac{1}{2x_r}\left[\ln\frac{(\sqrt{1+X_2^2}+X_2)}{(\sqrt{1+X_2^2}-X_2)} - \ln\frac{(\sqrt{1+X_1^2}+X_1)}{(\sqrt{1+X_1^2}-X_1)}\right]\right.$$

$$\left. - \frac{1}{x_2 - x_1}\ln\frac{(x_2+\sqrt{x_2^2+d^2})}{(x_1+\sqrt{x_1^2+d^2})}\ln\frac{(\sqrt{(x_r-x_2)^2+d^2}+x_2-x_r)}{(\sqrt{(x_r-x_1)^2+d^2}+x_1-x_r)}\right\}$$

D.15

APPENDIX E

TABULATION OF FENCE EFFECTS

FENCE EFFECT ON RESISTIVITY PROFILES
FENCE RESISTIVITY= 10*APPARENT RESISTIVITY
5000 FOOT DIPOLES, SENDER AT -5000 TO 0
RECEIVER AT 5000 TO 10000
FENCE AT X2 TO X2-L PARALLEL TO PROFILE LINE
DISTANCE OF FENCE TO PROFILE LINE= 10.

X2 L=	100	300	1000	3000	10000	30000	100000
-3000.	0.000	0.000	0.000	0.011	-0.024	-0.057	-0.080
-1000.	0.000	0.000	0.000	0.004	0.017	-0.045	-0.082
-300.	0.000	0.000	0.001	0.006	0.073	-0.026	-0.077
-100.	0.000	0.000	0.001	0.011	0.126	-0.007	-0.072
-30.	0.000	0.000	0.003	0.017	0.185	0.013	-0.066
-10.	0.001	-0.001	0.003	0.020	0.231	0.029	-0.062
0.	0.110	0.111	0.115	0.137	0.387	0.156	0.054
10.	0.222	0.223	0.228	0.253	0.543	0.283	0.170
30.	0.220	0.222	0.228	0.257	0.589	0.299	0.174
100.	0.110	0.221	0.228	0.261	0.648	0.320	0.181
300.	0.000	0.109	0.225	0.258	0.702	0.340	0.187
1000.	0.000	-0.000	0.105	0.236	0.754	0.362	0.196
3000.	0.000	-0.000	-0.000	0.083	0.755	0.380	0.207
9900.	0.000	0.000	0.000	0.000	-0.428	0.011	0.005
30000.	0.000	0.000	0.000	0.000	0.000	-0.156	0.001

FENCE EFFECT ON RESISTIVITY PROFILES
FENCE RESISTIVITY= 10*APPARENT RESISTIVITY
5000 FOOT DIPOLES, SENDER AT -5000 TO 0
RECEIVER AT 10000 TO 15000
FENCE AT X2 TO X2-L PARALLEL TO PROFILE LINE
DISTANCE OF FENCE TO PROFILE LINE= 10.

X2 L=	100	300	1000	3000	10000	30000	100000
-3000.	0.000	0.000	0.000	0.002	-0.008	-0.023	-0.036
-1000.	0.000	0.000	0.000	0.000	-0.000	-0.019	-0.035
-300.	0.000	0.000	0.000	0.001	0.004	-0.015	-0.032
-100.	0.000	0.000	0.000	0.001	0.007	-0.013	-0.028
-30.	0.000	0.000	0.000	0.001	0.008	-0.010	-0.025
-10.	0.000	0.000	0.000	0.002	0.010	-0.008	-0.022
0.	0.000	0.000	0.001	0.002	0.011	-0.006	-0.019
10.	0.000	0.000	0.001	0.003	0.012	-0.004	-0.017
30.	0.000	0.000	0.001	0.003	0.013	-0.002	-0.014
100.	0.000	0.000	0.001	0.004	0.015	0.000	-0.010
300.	0.000	-0.000	0.001	0.004	0.017	0.003	-0.007
1000.	0.000	-0.000	-0.001	0.002	0.022	0.007	-0.003
3000.	0.000	0.000	-0.000	-0.003	0.042	0.016	0.000
9900.	0.000	-0.000	-0.000	-0.001	-0.008	0.291	0.154
30000.	0.000	0.000	0.000	0.000	0.000	-0.114	0.001

FENCE EFFECT ON RESISTIVITY PROFILES
FENCE RESISTIVITY= 10*APPARENT RESISTIVITY
5000 FOOT DIPOLES, SENDER AT -5000 TO 0
RECEIVER AT 15000 TO 20000
FENCE AT X2 TO X2-L PARALLEL TO PROFILE LINE
DISTANCE OF FENCE TO PROFILE LINE= 10.

X2 L=	100	300	1000	3000	10000	30000	100000
-3000.	0.000	0.000	0.000	0.001	-0.004	-0.013	-0.022
-1000.	0.000	0.000	0.000	0.000	-0.001	-0.010	-0.021
-300.	0.000	0.000	0.000	0.000	0.001	-0.009	-0.019
-100.	0.000	0.000	0.000	0.000	0.002	-0.007	-0.017
-30.	0.000	0.000	0.000	0.001	0.003	-0.006	-0.015
-10.	0.000	0.000	0.000	0.001	0.004	-0.005	-0.013
0.	0.000	0.000	0.000	0.001	0.005	-0.004	-0.011
10.	0.000	0.000	0.000	0.001	0.005	-0.002	-0.010
30.	0.000	0.000	0.000	0.001	0.006	-0.001	-0.008
100.	0.000	0.000	0.000	0.002	0.007	0.000	-0.006
300.	0.000	-0.000	0.000	0.002	0.007	0.002	-0.004
1000.	0.000	-0.000	-0.000	0.001	0.009	0.003	-0.002
3000.	0.000	-0.000	-0.000	-0.001	0.013	0.006	0.000
9900.	0.000	0.000	0.000	0.000	-0.010	0.069	0.016
30000.	0.000	0.000	0.000	0.000	0.000	-0.125	0.002

FENCE EFFECT ON RESISTIVITY PROFILES
FENCE RESISTIVITY= 10*APPARENT RESISTIVITY
5000 FOOT DIPOLES, SENDER AT -5000 TO 0
RECEIVER AT 20000 TO 25000
FENCE AT X2 TO X2-L PARALLEL TO PROFILE LINE
DISTANCE OF FENCE TO PROFILE LINE= 10.

X2 L=	100	300	1000	3000	10000	30000	100000
-3000.	0.000	0.000	0.000	0.001	-0.003	-0.008	-0.015
-1000.	0.000	0.000	0.000	0.000	-0.000	-0.007	-0.014
-300.	0.000	0.000	0.000	0.000	0.001	-0.006	-0.013
-100.	0.000	0.000	0.000	0.000	0.001	-0.005	-0.012
-30.	0.000	0.000	0.000	0.000	0.002	-0.004	-0.010
-10.	0.000	0.000	0.000	0.001	0.002	-0.003	-0.009
0.	0.000	0.000	0.000	0.001	0.003	-0.002	-0.008
10.	0.000	0.000	0.000	0.001	0.003	-0.002	-0.007
30.	0.000	0.000	0.000	0.001	0.003	-0.001	-0.005
100.	0.000	0.000	0.000	0.001	0.004	0.000	-0.004
300.	0.000	-0.000	0.000	0.001	0.004	0.001	-0.003
1000.	0.000	-0.000	-0.000	0.000	0.005	0.002	-0.001
3000.	0.000	-0.000	-0.000	-0.001	0.007	0.004	0.000
9900.	0.000	0.000	0.000	0.000	-0.006	0.010	0.003
30000.	0.000	0.000	0.000	0.000	-0.031	-0.128	0.003

FENCE EFFECT ON RESISTIVITY PROFILES
FENCE RESISTIVITY= 10*APPARENT RESISTIVITY
5000 FOOT DIPOLES, SENDER AT -5000 TO 0
RECEIVER AT 5000 TO 10000
FENCE AT X2 TO X2-L PARALLEL TO PROFILE LINE
DISTANCE OF FENCE TO PROFILE LINE= 30.

X2 L=	100	300	1000	3000	10000	30000	100000
-3000.	0.000	0.000	0.000	0.009	-0.020	-0.047	-0.066
-1000.	0.000	0.000	0.000	0.004	0.014	-0.038	-0.068
-300.	0.000	0.000	0.001	0.006	0.059	-0.022	-0.065
-100.	0.000	-0.000	0.001	0.011	0.102	-0.007	-0.061
-30.	0.001	-0.001	0.001	0.014	0.144	0.007	-0.058
-10.	0.006	-0.005	-0.003	0.013	0.163	0.011	-0.059
0.	0.093	0.093	0.096	0.113	0.275	0.114	0.040
10.	0.191	0.191	0.195	0.213	0.387	0.217	0.140
30.	0.187	0.187	0.191	0.211	0.405	0.221	0.139
100.	0.093	0.186	0.190	0.214	0.447	0.236	0.142
300.	0.000	0.092	0.188	0.213	0.491	0.252	0.148
1000.	0.000	-0.000	0.089	0.198	0.534	0.271	0.155
3000.	0.000	-0.000	-0.000	0.072	0.537	0.287	0.166
9900.	0.000	0.000	0.000	0.000	-0.262	0.009	0.004
30000.	0.000	0.000	0.000	0.000	0.000	-0.114	0.001

FENCE EFFECT ON RESISTIVITY PROFILES
FENCE RESISTIVITY= 10*APPARENT RESISTIVITY
5000 FOOT DIPOLES, SENDER AT -5000 TO 0
RECEIVER AT 10000 TO 15000
FENCE AT X2 TO X2-L PARALLEL TO PROFILE LINE
DISTANCE OF FENCE TO PROFILE LINE= 30.

X2 L=	100	300	1000	3000	10000	30000	100000
-3000.	0.000	0.000	0.000	0.002	-0.007	-0.018	-0.029
-1000.	0.000	0.000	0.000	0.000	-0.000	-0.015	-0.028
-300.	0.000	0.000	0.000	0.001	0.004	-0.012	-0.025
-100.	0.000	0.000	0.000	0.001	0.006	-0.010	-0.022
-30.	0.000	0.000	0.000	0.001	0.007	-0.007	-0.019
-10.	0.000	0.000	0.000	0.002	0.008	-0.006	-0.018
0.	0.000	0.000	0.000	0.002	0.009	-0.006	-0.017
10.	0.000	0.000	0.000	0.002	0.009	-0.005	-0.016
30.	0.000	0.000	0.001	0.002	0.010	-0.004	-0.014
100.	0.000	0.000	0.001	0.003	0.011	-0.001	-0.011
300.	0.000	-0.000	0.000	0.003	0.013	0.001	-0.008
1000.	0.000	-0.000	-0.000	0.001	0.018	0.005	-0.004
3000.	0.000	0.000	-0.000	-0.002	0.034	0.013	-0.001
9900.	0.000	0.000	-0.000	-0.001	0.005	0.214	0.123
30000.	0.000	0.000	0.000	0.000	0.000	-0.078	0.001

FENCE EFFECT ON RESISTIVITY PROFILES
FENCE RESISTIVITY= 10*APPARENT RESISTIVITY
5000 FOOT DIPOLES, SENDER AT -5000 TO 0
RECEIVER AT 15000 TO 20000
FENCE AT X2 TO X2-L PARALLEL TO PROFILE LINE
DISTANCE OF FENCE TO PROFILE LINE= 30.

X2 L=	100	300	1000	3000	10000	30000	100000
-3000.	0.000	0.000	0.000	0.001	-0.003	-0.010	-0.018
-1000.	0.000	0.000	0.000	0.000	-0.000	-0.009	-0.017
-300.	0.000	0.000	0.000	0.000	0.001	-0.007	-0.015
-100.	0.000	0.000	0.000	0.000	0.002	-0.005	-0.013
-30.	0.000	0.000	0.000	0.001	0.003	-0.004	-0.011
-10.	0.000	0.000	0.000	0.001	0.003	-0.003	-0.010
0.	0.000	0.000	0.000	0.001	0.004	-0.003	-0.010
10.	0.000	0.000	0.000	0.001	0.004	-0.003	-0.009
30.	0.000	0.000	0.000	0.001	0.004	-0.002	-0.008
100.	0.000	0.000	0.000	0.001	0.005	-0.001	-0.006
300.	0.000	-0.000	0.000	0.001	0.006	0.001	-0.004
1000.	0.000	-0.000	-0.000	0.001	0.007	0.002	-0.002
3000.	0.000	-0.000	-0.000	-0.001	0.010	0.005	-0.000
9900.	0.000	-0.000	0.000	0.000	-0.006	0.058	0.013
30000.	0.000	0.000	0.000	0.000	0.000	-0.088	0.002

FENCE EFFECT ON RESISTIVITY PROFILES
FENCE RESISTIVITY= 10*APPARENT RESISTIVITY
5000 FOOT DIPOLES, SENDER AT -5000 TO 0
RECEIVER AT 20000 TO 25000
FENCE AT X2 TO X2-L PARALLEL TO PROFILE LINE
DISTANCE OF FENCE TO PROFILE LINE= 30.

X2 L=	100	300	1000	3000	10000	30000	100000
-3000.	0.000	0.000	0.000	0.000	-0.002	-0.007	-0.012
-1000.	0.000	0.000	0.000	0.000	-0.000	-0.005	-0.012
-300.	0.000	0.000	0.000	0.000	0.001	-0.004	-0.010
-100.	0.000	0.000	0.000	0.000	0.001	-0.003	-0.009
-30.	0.000	0.000	0.000	0.000	0.002	-0.003	-0.008
-10.	0.000	0.000	0.000	0.000	0.002	-0.002	-0.007
0.	0.000	0.000	0.000	0.000	0.002	-0.002	-0.007
10.	0.000	0.000	0.000	0.001	0.002	-0.002	-0.006
30.	0.000	0.000	0.000	0.001	0.002	-0.001	-0.005
100.	0.000	0.000	0.000	0.001	0.003	-0.000	-0.004
300.	0.000	-0.000	0.000	0.001	0.003	0.000	-0.003
1000.	0.000	-0.000	-0.000	0.000	0.004	0.002	-0.001
3000.	0.000	-0.000	-0.000	-0.001	0.005	0.003	-0.000
9900.	0.000	0.000	0.000	0.000	-0.005	0.008	0.002
30000.	0.000	0.000	0.000	0.000	-0.027	-0.091	0.002

FENCE EFFECT ON RESISTIVITY PROFILES
FENCE RESISTIVITY= 10*APPARENT RESISTIVITY
5000 FOOT DIPOLES, SENDER AT -5000 TO 0
RECEIVER AT 5000 TO 10000
FENCE AT X2 TO X2-L PARALLEL TO PROFILE LINE
DISTANCE OF FENCE TO PROFILE LINE= 100.

X2 L=	100	300	1000	3000	10000	30000	100000
-3000.	0.000	0.000	0.000	0.006	-0.015	-0.035	-0.050
-1000.	0.000	-0.000	0.000	0.004	0.010	-0.030	-0.053
-300.	0.000	-0.000	0.000	0.006	0.043	-0.018	-0.052
-100.	0.001	-0.001	-0.000	0.008	0.071	-0.009	-0.050
-30.	0.005	-0.006	-0.005	0.006	0.084	-0.007	-0.053
-10.	0.012	-0.013	-0.012	-0.001	0.083	-0.012	-0.060
0.	0.075	0.074	0.075	0.087	0.174	0.076	0.028
10.	0.162	0.161	0.162	0.174	0.264	0.164	0.115
30.	0.156	0.153	0.155	0.168	0.263	0.159	0.109
100.	0.075	0.149	0.151	0.165	0.276	0.161	0.106
300.	0.000	0.074	0.149	0.165	0.305	0.171	0.109
1000.	0.000	-0.000	0.072	0.155	0.338	0.186	0.115
3000.	0.000	-0.000	-0.000	0.060	0.341	0.200	0.125
9900.	0.000	0.000	0.000	0.000	-0.127	0.007	0.003
30000.	0.000	0.000	0.000	0.000	0.000	-0.076	0.001

FENCE EFFECT ON RESISTIVITY PROFILES
FENCE RESISTIVITY= 10*APPARENT RESISTIVITY
5000 FOOT DIPOLES, SENDER AT -5000 TO 0
RECEIVER AT 10000 TO 15000
FENCE AT X2 TO X2-L PARALLEL TO PROFILE LINE
DISTANCE OF FENCE TO PROFILE LINE= 100.

X2 L=	100	300	1000	3000	10000	30000	100000
-3000.	0.000	0.000	0.000	0.001	-0.005	-0.014	-0.022
-1000.	0.000	0.000	0.000	0.000	-0.000	-0.012	-0.022
-300.	0.000	0.000	0.000	0.001	0.003	-0.009	-0.019
-100.	0.000	0.000	0.000	0.001	0.005	-0.007	-0.016
-30.	0.000	0.000	0.000	0.001	0.006	-0.005	-0.014
-10.	0.000	0.000	0.000	0.001	0.006	-0.005	-0.014
0.	0.000	0.000	0.000	0.001	0.006	-0.005	-0.014
10.	0.000	0.000	0.000	0.001	0.006	-0.004	-0.013
30.	0.000	0.000	0.000	0.001	0.007	-0.004	-0.013
100.	0.000	0.000	0.000	0.002	0.008	-0.003	-0.011
300.	0.000	-0.000	0.000	0.002	0.009	-0.001	-0.008
1000.	0.000	-0.000	-0.000	0.001	0.013	0.003	-0.005
3000.	0.000	-0.000	-0.000	-0.002	0.025	0.009	-0.002
9900.	0.001	0.001	0.001	-0.000	0.021	0.146	0.094
30000.	0.000	0.000	0.000	0.000	0.000	-0.047	0.001

FENCE EFFECT ON RESISTIVITY PROFILES
FENCE RESISTIVITY= 10*APPARENT RESISTIVITY
5000 FOOT DIPOLES, SENDER AT -5000 TO 0
RECEIVER AT 15000 TO 20000
FENCE AT X2 TO X2-L PARALLEL TO PROFILE LINE
DISTANCE OF FENCE TO PROFILE LINE= 100.

X2 L=	100	300	1000	3000	10000	30000	100000
-3000.	0.000	0.000	0.000	0.000	-0.002	-0.008	-0.013
-1000.	0.000	0.000	0.000	0.000	-0.000	-0.006	-0.013
-300.	0.000	0.000	0.000	0.000	0.001	-0.005	-0.011
-100.	0.000	0.000	0.000	0.000	0.002	-0.004	-0.009
-30.	0.000	0.000	0.000	0.001	0.002	-0.003	-0.008
-10.	0.000	0.000	0.000	0.001	0.003	-0.003	-0.008
0.	0.000	0.000	0.000	0.001	0.003	-0.003	-0.008
10.	0.000	0.000	0.000	0.001	0.003	-0.002	-0.008
30.	0.000	0.000	0.000	0.001	0.003	-0.002	-0.007
100.	0.000	0.000	0.000	0.001	0.003	-0.001	-0.006
300.	0.000	-0.000	0.000	0.001	0.004	-0.000	-0.005
1000.	0.000	-0.000	-0.000	0.000	0.005	0.001	-0.003
3000.	0.000	-0.000	-0.000	-0.001	0.008	0.004	-0.001
9900.	0.000	-0.000	-0.000	-0.000	-0.003	0.043	0.008
30000.	0.000	0.000	0.000	0.000	0.000	-0.055	0.001

FENCE EFFECT ON RESISTIVITY PROFILES
FENCE RESISTIVITY= 10*APPARENT RESISTIVITY
5000 FOOT DIPOLES, SENDER AT -5000 TO 0
RECEIVER AT 20000 TO 25000
FENCE AT X2 TO X2-L PARALLEL TO PROFILE LINE
DISTANCE OF FENCE TO PROFILE LINE= 100.

X2 L=	100	300	1000	3000	10000	30000	100000
-3000.	0.000	0.000	0.000	0.000	-0.001	-0.005	-0.009
-1000.	0.000	0.000	0.000	0.000	-0.000	-0.004	-0.009
-300.	0.000	0.000	0.000	0.000	0.001	-0.003	-0.008
-100.	0.000	0.000	0.000	0.000	0.001	-0.002	-0.006
-30.	0.000	0.000	0.000	0.000	0.001	-0.002	-0.006
-10.	0.000	0.000	0.000	0.000	0.001	-0.002	-0.005
0.	0.000	0.000	0.000	0.000	0.001	-0.002	-0.005
10.	0.000	0.000	0.000	0.000	0.002	-0.002	-0.005
30.	0.000	0.000	0.000	0.000	0.002	-0.001	-0.005
100.	0.000	0.000	0.000	0.000	0.002	-0.001	-0.004
300.	0.000	-0.000	0.000	0.000	0.002	-0.000	-0.003
1000.	0.000	-0.000	-0.000	0.000	0.003	0.001	-0.002
3000.	0.000	-0.000	-0.000	-0.000	0.004	0.002	-0.000
9900.	0.000	-0.000	0.000	0.000	-0.003	0.007	0.002
30000.	0.000	0.000	0.000	0.000	-0.023	-0.057	0.002

FENCE EFFECT ON RESISTIVITY PROFILES
FENCE RESISTIVITY= 10*APPARENT RESISTIVITY
5000 FOOT DIPOLES, SENDER AT -5000 TO 0
RECEIVER AT 5000 TO 10000
FENCE AT X2 TO X2-L PARALLEL TO PROFILE LINE
DISTANCE OF FENCE TO PROFILE LINE= 300.

X2 L=	100	300	1000	3000	10000	30000	100000
-3000.	0.000	-0.000	0.000	0.003	-0.010	-0.025	-0.036
-1000.	0.000	-0.000	-0.000	0.003	0.006	-0.022	-0.040
-300.	0.001	-0.001	-0.001	0.004	0.025	-0.017	-0.041
-100.	0.003	-0.005	-0.005	0.001	0.033	-0.017	-0.044
-30.	0.009	-0.013	-0.013	-0.007	0.030	-0.023	-0.051
-10.	0.017	-0.021	-0.021	-0.015	0.023	-0.030	-0.059
0.	0.062	0.057	0.056	0.063	0.102	0.048	0.018
10.	0.140	0.135	0.134	0.141	0.180	0.126	0.096
30.	0.133	0.127	0.126	0.133	0.173	0.118	0.088
100.	0.062	0.120	0.118	0.125	0.171	0.112	0.081
300.	0.001	0.058	0.114	0.122	0.179	0.113	0.079
1000.	0.000	-0.000	0.056	0.116	0.199	0.123	0.082
3000.	0.000	0.000	-0.000	0.049	0.203	0.135	0.091
9900.	0.000	0.000	0.000	0.000	-0.047	0.005	0.002
30000.	0.000	0.000	0.000	0.000	0.000	-0.048	0.001

FENCE EFFECT ON RESISTIVITY PROFILES
FENCE RESISTIVITY= 10*APPARENT RESISTIVITY
5000 FOOT DIPOLES, SENDER AT -5000 TO 0
RECEIVER AT 10000 TO 15000
FENCE AT X2 TO X2-L PARALLEL TO PROFILE LINE
DISTANCE OF FENCE TO PROFILE LINE= 300.

X2 L=	100	300	1000	3000	10000	30000	100000
-3000.	0.000	-0.000	0.000	0.001	-0.003	-0.010	-0.016
-1000.	0.000	0.000	0.000	0.000	0.000	-0.008	-0.015
-300.	0.000	0.000	0.000	0.001	0.002	-0.006	-0.013
-100.	0.000	0.000	0.000	0.001	0.003	-0.005	-0.012
-30.	0.000	0.000	0.000	0.001	0.004	-0.004	-0.011
-10.	0.000	0.000	0.000	0.001	0.004	-0.004	-0.011
0.	0.000	0.000	0.000	0.001	0.004	-0.004	-0.011
10.	0.000	0.000	0.000	0.001	0.004	-0.004	-0.011
30.	0.000	0.000	0.000	0.001	0.004	-0.004	-0.010
100.	0.000	0.000	0.000	0.001	0.005	-0.003	-0.010
300.	0.000	-0.000	0.000	0.001	0.006	-0.002	-0.008
1000.	0.000	-0.000	-0.000	0.001	0.009	0.001	-0.005
3000.	0.000	-0.000	-0.000	-0.001	0.017	0.006	-0.003
9900.	0.002	0.002	0.003	0.002	0.035	0.102	0.073
30000.	0.000	0.000	0.000	0.000	0.000	-0.025	0.001

FENCE EFFECT ON RESISTIVITY PROFILES
FENCE RESISTIVITY= 10*APPARENT RESISTIVITY
5000 FOOT DIPOLES, SENDER AT -5000 TO 0
RECEIVER AT 15000 TO 20000
FENCE AT X2 TO X2-L PARALLEL TO PROFILE LINE
DISTANCE OF FENCE TO PROFILE LINE= 300.

X2 L=	100	300	1000	3000	10000	30000	100000
-3000.	0.000	0.000	0.000	0.000	-0.002	-0.005	-0.010
-1000.	0.000	0.000	0.000	0.000	-0.000	-0.004	-0.009
-300.	0.000	0.000	0.000	0.000	0.001	-0.003	-0.008
-100.	0.000	0.000	0.000	0.000	0.001	-0.002	-0.007
-30.	0.000	0.000	0.000	0.000	0.002	-0.002	-0.006
-10.	0.000	0.000	0.000	0.000	0.002	-0.002	-0.006
0.	0.000	0.000	0.000	0.000	0.002	-0.002	-0.006
10.	0.000	0.000	0.000	0.000	0.002	-0.002	-0.006
30.	0.000	0.000	0.000	0.000	0.002	-0.002	-0.006
100.	0.000	0.000	0.000	0.000	0.002	-0.002	-0.006
300.	0.000	-0.000	0.000	0.000	0.002	-0.001	-0.005
1000.	0.000	-0.000	-0.000	0.000	0.004	0.000	-0.003
3000.	0.000	-0.000	-0.000	-0.000	0.005	0.002	-0.001
9900.	0.001	-0.002	-0.002	-0.002	-0.003	0.026	0.003
30000.	0.000	0.000	0.000	0.000	0.000	-0.031	0.001

FENCE FFFECT ON RESISTIVITY PROFILES
FENCE RESISTIVITY= 10*APPARENT RESISTIVITY
5000 FOOT DIPOLES, SENDER AT -5000 TO 0
RECEIVER AT 20000 TO 25000
FENCE AT X2 TO X2-L PARALLEL TO PROFILE LINE
DISTANCE OF FENCE TO PROFILE LINE= 300.

X2 L=	100	300	1000	3000	10000	30000	100000
-3000.	0.000	0.000	0.000	0.000	-0.001	-0.003	-0.007
-1000.	0.000	0.000	0.000	0.000	-0.000	-0.003	-0.006
-300.	0.000	0.000	0.000	0.000	0.001	-0.002	-0.005
-100.	0.000	0.000	0.000	0.000	0.001	-0.002	-0.004
-30.	0.000	0.000	0.000	0.000	0.001	-0.001	-0.004
-10.	0.000	0.000	0.000	0.000	0.001	-0.001	-0.004
0.	0.000	0.000	0.000	0.000	0.001	-0.001	-0.004
10.	0.000	0.000	0.000	0.000	0.001	-0.001	-0.004
30.	0.000	0.000	0.000	0.000	0.001	-0.001	-0.004
100.	0.000	0.000	0.000	0.000	0.001	-0.001	-0.004
300.	0.000	-0.000	0.000	0.000	0.001	-0.001	-0.003
1000.	0.000	-0.000	-0.000	0.000	0.002	0.000	-0.002
3000.	0.000	-0.000	-0.000	-0.000	0.003	0.001	-0.001
9900.	0.000	-0.000	-0.000	0.000	-0.002	0.005	0.001
30000.	0.000	0.000	0.000	0.000	-0.010	-0.033	0.001

FENCE EFFECT ON RESISTIVITY PROFILES
FENCE RESISTIVITY= 10*APPARENT RESISTIVITY
5000 FOOT DIPOLES, SENDER AT -5000 TO 0
RECEIVER AT 5000 TO 10000
FENCE AT X2 TO X2-L PARALLEL TO PROFILE LINE
DISTANCE OF FENCE TO PROFILE LINE=1000.

X2 L=	100	300	1000	3000	10000	30000	100000
-3000.	0.000	-0.000	-0.000	-0.000	-0.006	-0.014	-0.021
-1000.	0.000	-0.001	-0.001	-0.000	-0.001	-0.016	-0.027
-300.	0.002	-0.004	-0.006	-0.005	-0.000	-0.019	-0.032
-100.	0.005	-0.009	-0.013	-0.013	-0.006	-0.026	-0.039
-30.	0.011	-0.017	-0.022	-0.022	-0.014	-0.035	-0.048
-10.	0.018	-0.025	-0.031	-0.030	-0.022	-0.043	-0.057
0.	0.050	0.043	0.038	0.038	0.046	0.025	0.011
10.	0.119	0.111	0.106	0.106	0.114	0.093	0.079
30.	0.113	0.103	0.097	0.098	0.106	0.085	0.071
100.	0.051	0.096	0.089	0.089	0.098	0.076	0.062
300.	0.002	0.044	0.083	0.082	0.093	0.071	0.056
1000.	0.000	-0.001	0.039	0.077	0.096	0.070	0.053
3000.	0.000	0.000	0.000	0.037	0.098	0.078	0.060
9900.	0.000	0.000	0.000	0.000	0.003	0.003	0.001
30000.	0.000	0.000	0.000	0.000	0.000	-0.025	0.001

FENCE FFFECT ON RFSISTIVITY PROFILES
FENCE RESISTIVITY= 10*APPARENT RESISTIVITY
5000 FOOT DIPOLES, SENDER AT -5000 TO 0
RECEIVER AT 10000 TO 15000
FENCE AT X2 TO X2-L PARALLEL TO PROFILE LINE
DISTANCE OF FENCE TO PROFILE LINE=1000.

X2 L=	100	300	1000	3000	10000	30000	100000
-3000.	0.000	-0.000	-0.000	0.000	-0.002	-0.005	-0.009
-1000.	0.000	-0.000	0.000	0.000	0.000	-0.005	-0.009
-300.	0.000	0.000	0.000	0.000	0.001	-0.004	-0.008
-100.	0.000	0.000	0.000	0.000	0.002	-0.003	-0.008
-30.	0.000	0.000	0.000	0.000	0.002	-0.003	-0.008
-10.	0.000	0.000	0.000	0.000	0.002	-0.003	-0.008
0.	0.000	0.000	0.000	0.000	0.002	-0.003	-0.008
10.	0.000	0.000	0.000	0.000	0.002	-0.003	-0.007
30.	0.000	0.000	0.000	0.000	0.002	-0.003	-0.007
100.	0.000	0.000	0.000	0.000	0.002	-0.003	-0.007
300.	0.000	0.000	0.000	0.000	0.002	-0.002	-0.007
1000.	0.000	-0.000	-0.000	0.000	0.004	-0.001	-0.006
3000.	0.000	-0.000	-0.000	-0.000	0.008	0.002	-0.004
9900.	0.002	0.004	0.006	0.007	0.043	0.068	0.055
30000.	0.000	0.000	0.000	0.000	0.000	-0.009	0.001

FENCE EFFECT ON RESISTIVITY PROFILES
FENCE RESISTIVITY= 10*APPARENT RESISTIVITY
5000 FOOT DIPOLES, SENDER AT -5000 TO 0
RECEIVER AT 15000 TO 20000
FENCE AT X2 TO X2-L PARALLEL TO PROFILE LINE
DISTANCE OF FENCE TO PROFILE LINE=1000.

X2 L=	100	300	1000	3000	10000	30000	100000
-3000.	0.000	-0.000	-0.000	0.000	-0.001	-0.003	-0.005
-1000.	0.000	0.000	0.000	0.000	0.000	-0.002	-0.005
-300.	0.000	0.000	0.000	0.000	0.001	-0.002	-0.005
-100.	0.000	0.000	0.000	0.000	0.001	-0.002	-0.004
-30.	0.000	0.000	0.000	0.000	0.001	-0.001	-0.004
-10.	0.000	0.000	0.000	0.000	0.001	-0.001	-0.004
0.	0.000	0.000	0.000	0.000	0.001	-0.001	-0.004
10.	0.000	0.000	0.000	0.000	0.001	-0.001	-0.004
30.	0.000	0.000	0.000	0.000	0.001	-0.001	-0.004
100.	0.000	0.000	0.000	0.000	0.001	-0.001	-0.004
300.	0.000	0.000	0.000	0.000	0.001	-0.001	-0.004
1000.	0.000	0.000	0.000	0.000	0.002	-0.000	-0.003
3000.	0.000	-0.000	-0.000	-0.000	0.003	0.001	-0.002
9900.	0.002	-0.003	-0.004	-0.004	-0.005	0.008	-0.004
30000.	0.000	0.000	0.000	0.000	0.000	-0.013	0.001

FENCE EFFECT ON RESISTIVITY PROFILES
FENCE RESISTIVITY= 10*APPARENT RESISTIVITY
5000 FOOT DIPOLES, SENDER AT -5000 TO 0
RECEIVER AT 20000 TO 25000
FENCE AT X2 TO X2-L PARALLEL TO PROFILE LINE
DISTANCE OF FENCE TO PROFILE LINE=1000.

X2 L=	100	300	1000	3000	10000	30000	100000
-3000.	0.000	-0.000	0.000	0.000	-0.000	-0.002	-0.004
-1000.	0.000	0.000	0.000	0.000	0.000	-0.001	-0.004
-300.	0.000	0.000	0.000	0.000	0.000	-0.001	-0.003
-100.	0.000	0.000	0.000	0.000	0.000	-0.001	-0.003
-30.	0.000	0.000	0.000	0.000	0.000	-0.001	-0.003
-10.	0.000	0.000	0.000	0.000	0.000	-0.001	-0.003
0.	0.000	0.000	0.000	0.000	0.000	-0.001	-0.003
10.	0.000	0.000	0.000	0.000	0.000	-0.001	-0.003
30.	0.000	0.000	0.000	0.000	0.000	-0.001	-0.003
100.	0.000	0.000	0.000	0.000	0.001	-0.001	-0.003
300.	0.000	0.000	0.000	0.000	0.001	-0.001	-0.002
1000.	0.000	0.000	0.000	0.000	0.001	-0.000	-0.002
3000.	0.000	0.000	-0.000	-0.000	0.001	0.001	-0.001
9900.	0.000	-0.000	-0.000	-0.000	-0.001	0.003	0.000
30000.	0.000	0.000	0.000	0.000	-0.014	-0.014	0.001

BIBLIOGRAPHY

Emerson, B.K., 1917; Geology of Massachusetts and Rhode Island, U.S.G.S. Bulletin, No. 597.

Franklin, , 1944 Methods of Advanced Calculus, John Wiley and Co.

Hallof, P.G., 1957; On the Interpretation of Resistivity and Induced Polarization Results; Ph.D. Thesis, M.I.T.

Hauck, A.M., 1960; Deep Resistivity Measurements in Massachusetts; M.S. Thesis, M.I.T.

Lee, Y.W., 1960; Statistical Theory of Communication; John Wiley and Sons, Inc., New York.

Madden, T.R., Thompson, W.B., and Hauck, A.M., 1960; AMT-2; Audio Magneto-Tellurics Progress Report No. 2; Geology Department, M.I.T.

Ness, N.F., 1959; Resistivity Interpretation in Geophysical Prospecting, Ph.D. Thesis, M.I.T.

Regier, A.A., 1962; Deep Resistivity Measurements along the Massachusetts Turnpike, B.S. Thesis, M.I.T.

La Compagnie General de Geophysique, 1955; Abaques de sondage Electrique; Geophys. Prosp., III, Supplement No. 3.